IMAGE: A MAP OF THE STARS OF THE ORION CONSTELLATION

Print ISSN: 2631-8490 Online ISSN: 2631-8504

JournalPreview

London Journal of Research in Science: Natural and Formal
Volume 21 | Issue 3 | Compilation 1.0

London Journals Press

Journal Content
In this Issue

London Journals Press

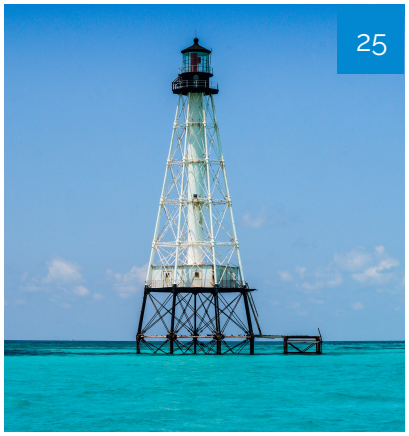

Underlying Structure-Activity Correlations of 2d Layered Transition Metal Dichalcogenides based Electrocatalysts for Boosted Hydrogen Generation

Zhexu Xi

University of Bristol

ABSTRACT

Hydrogen fuel is an ideal energy source to replace the traditional fossil fuels because of its high energy density and renewability. Electrocemical water splitting is also regarded as a sustainable, cleaning and eco-friendly method for hydrogen evolution reaction (HER), but a cheaper, earth-abundant and similarly efficient alternative to Pt as an HER catalyst cannot still be discovered. Recently, 2D Transition Metal Dichalcogenides (TMDs) are demonstrated to greatly enhance the HER activity. Herein, our work provides an insight into the recent advances in 2D TMDs-based HER following the Composition-characterisation-construction guideline. After the background introduction, several research outputs based on 2D TMDs as well as the comprehensive analysis on the modulation strategies of 2D TMDs, for the purposes of increasing the active sites, improving the intrinsic activity and altering the electronic states. Finally, the future opportuni- ties and challenges of 2D TMDs electrocatalysts are briefly featured.

Keywords: electrocatalysts; transition metal dich- alcogenides; hydrogen evolution; modification; basel plane; active sites.

Classification: FOR Code: 091599

Language: English

London Journals Press

LJP Copyright ID: 925652
Print ISSN: 2631-8490
Online ISSN: 2631-8504

London Journal of Research in Science: Natural and Formal

Volume 21 | Issue 3 | Compilation 1.0

Underlying Structure-Activity Correlations of 2d Layered Transition Metal Dichalcogenides -based Electrocatalysts for Boosted Hydrogen Generation

Zhexu Xi

ABSTRACT

Hydrogen fuel is an ideal energy source to replace the traditional fossil fuels because of its high energy density and renewability. Electrocemical water splitting is also regarded as a sustainable, cleaning and eco-friendly method for hydrogen evolution reaction (HER), but a cheaper, earth-abundant and similarly efficient alternative to Pt as an HER catalyst cannot still be discovered. Recently, 2D Transition Metal Dichalcogenides (TMDs) are demonstrated to greatly enhance the HER activity. Herein, our work provides an insight into the recent advances in 2D TMDs-based HER following the Composition-characterisation-construction guideline. After the background introduction, several research outputs based on 2D TMDs as well as the comprehensive analysis on the modulation strategies of 2D TMDs, for the purposes of increasing the active sites, improving the intrinsic activity and altering the electronic states. Finally, the future opportunities and challenges of 2D TMDs electrocatalysts are briefly featured.

Keywords: electrocatalysts; transition metal dichalcogenides; hydrogen evolution; modification; basel plane; active sites.

Author: Bristol Centre for Functional Nanomaterials, University of Bristol, Bristol, UK.

I. INTRODUCTION

Nowadays, demand for usable energy worldwide has dramatically risen due to rapid growth in population, which inevitably triggers the overuse of traditional fossil fuels as well as a series of environmental issues[1, 2]. Accordingly, it is of great importance to find another, less polluting energy source to tackle the current problems. Hydrogen (H_2), owing to its zero - polluting combustion byproduct (water) and high energy density, holds high potential as an alternative to fossil energy[3]. For H_2 production pathways, water electrolysis (electrocatalytic water splitting) is also known as a renewable and clean industrial approach[4]. Currently, the best electrocatalyst for the Hydrogen Evolution Reaction (HER) is Pt, which markedly minimizes the overpotential and exhibits optimal catalytic activity.

However, the high cost and limited reserves of Pt seriously restrict the further development of Pt-based catalysts[3, 5]. Thus, a novel HER electrocatalyst with rich abundance and similar reactivity to Pt has captured wide attention.

Two-dimensional transition metal dichalcogenides (2D TMDs), also generally expressed in the form of MX_n (M = Mo, W, Ti, V, and Zr; X= S, Se, and Te), have recently been verified to be the most prospective promising alternatives to Pt due to extraordinary catalytic performance [4-6]. First, the atomically thin 2D layered structure offers plentiful exposed active sites and a high specific area for HER[3][7]. Second, the unique characteristics of TMDs are primarily related to the tailor-made electronic structures, which can provide a more accurate and comprehensive understanding in terms of their HER catalytic mechanisms[7, 8]. Third, although the unsatisfactory in-plane activity of TMDs has been reported to restrict the applications in HER electroca-

talysts, more strategies based on the structural modification of TMDs have been implemented to improve the catalytic performance, including phase transition and defect engineering[8, 9].

Herein, we focus on the role of 2D TMDs as ideal replacements for Pt in HER enhancement. First, we summarise the theoretical understanding of the overall electrocatalytic HER system. Second, based on the recent discoveries in this rapidly advancing research area, we make a comprehensive analysis regarding the nanoscale modulation strategies of 2D-TMDs-based electrocatalysts in three aspects: 1) composition (different kinds of 2D TMDs that have superior HER catalytic performance, as well as how structural modulation strategies are implemented), 2) characterisation (various instrumental techniques used for measurement, analysis and quantification of 2D TMDs), and 3) construction (novel nanoengineered 2D TMDs based on versatile modulation strategies that boost the HER activity)[3-5, 7-9, 10]. Finally, we propose the perspectives and challenges of TMDs-based electrochemical water splitting technologies, which can provide more insights into the rational design and fabrication of HER-related catalysts.

II. FUNDAMENTALS OF HER

For HER electrocatalysis, three elementary reactions are involved, including one discharge step and two different hydrogen desorption steps (chemical and electrochemical pathways). As Fig. 1 illustrates, a transferred electron initially forms an adsorbed hydrogen atom (H*) with a combination of a proton on the active site of the electrode surface (the Volmer or discharge reaction step), and then generates H_2 by combination with another adsorbed atom (the Tafel step) or a proton from the solution (the Heyrovsky step), which depends on the kind of the electrode material[11].

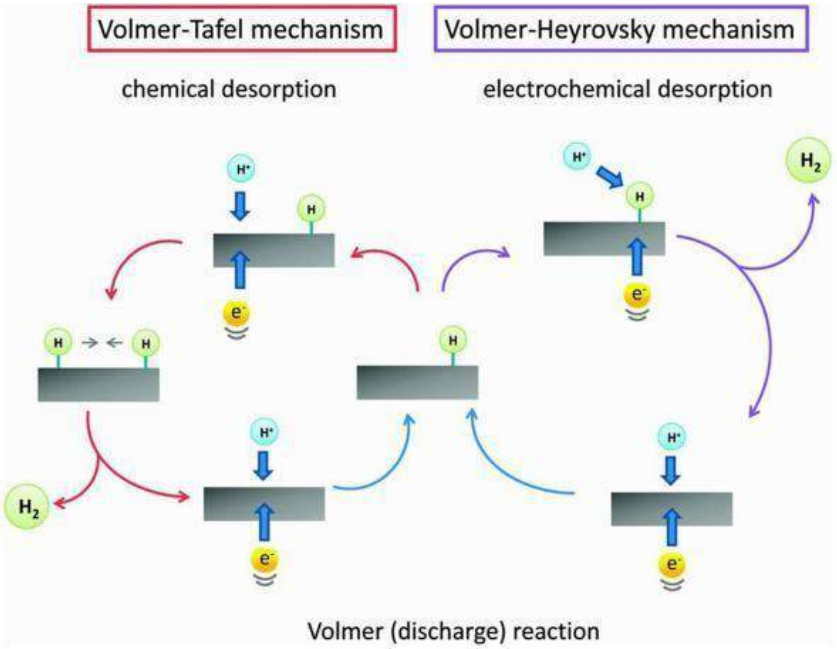

Figure 1: The mechanism of HER in acidic media[11]

Based on the HER process in acidic solutions, the critical parameter to thermodynamically control the entire catalytic reaction rate is the corresponding Gibbs Free Energy change for absorbed hydrogen atoms (ΔG_H), which is connected with the balance between the H* adsorption and H_2 desorption step. From the physical chemistry perspective, if the hydrogen-catalyst bonding on the electrode surface is too strong, making the Volmer step more straightforward, the desorption reaction will be the rate-determining step; otherwise, the initial Volmer step will be started with a tremendous driving force and accordingly, the adsorption will be the rate-determining

step[8]. Hence, a nearly zero value of ΔG_H can bring about the best HER performance, which has also become a constant focus of the optimal design of ideal TMD-based catalysts[8, 11].

III. GENERAL OUTLINE ON THE MODIFICATION STRATEGIES OF 2D TMDS FOR

3.1 Boosted HER performance

In the context of a comprehensive characterisation composition-construction analysis, different categories of nanolayered TMDs have been firmly demonstrated to be ideal for HER enhancement due to their appealing electronic properties and similar stacking methods, so they are naturally the largest families of functionalized catalysts for electrochemical reactions[7, 12].

In the 1970s, layered TMDs have been identified as unsuitable electrocatalysts for hydrogen generation due to the low intrinsic activity in the bulk state[13]. Until 2005, Hinnemann et al.[14] found that the Mo-edge of MoS_2 (1010) is similar to the HER active sites of nitrogenase. Simultaneously, their calculation based on a Density Functional Theory (DFT) model shows a comparable ΔG_H value to Pt, which theoretically predicts the excellent HER performance. Then, they loaded MoS_2 nanoparticles on the graphite substrate to experimentally confirm their predic- tion. More recent research identifies that the edge of MoS_2 plays a more vital role than its inert basal plane in electrocatalytic HER, even revealing the linear relationship between the HER activity and the edge length[15]. Therefore, three main modification routes emerge: 1) structural engineering: for the limited edge sites of TMDs, to increase the concentration of edge sites by regulating the architecture on the nanoscale; 2) edge/in-plane intrinsic activity regulation: to significantly activate the inherently inert basal plane or edge sites; and 3) to optimise the electronic structure of TMDs.

The first route focuses substantially on increasing the number of exposed active sites; the second route is to lessen the charge transfer resistance; the third route is even more valuable for the overall HER catalytic activity enhancement.

IV. INCREASING THE CONCENTRATION OF EDGE SITES

4.1 Physical Exfoliation from bulk materials

Compared with bulk materials, the most appealing trait for 2D-layered TMDs is a relatively big specific surface area, which provides plenty of rooms for adequately exposed active sites $_{\text{on edge}}$[10, 11].

To maximise the edge active sites in bulk state for enhanced HER activity, more well-tuned and various morphological features should be physically or chemically tuned. One direct and straight-forward physical method refers to thinning the thickness and numbers of layers. The typical approach is mechanical exfoliation from the bulk states to the monolayered TMD nanosheets. This easy way markedly contributes to the boosted HER activity, and more importantly, makes it easier for a better understanding of the entire HER experimental system. Accordingly, creating a TMD monolayer by exfoliation is widely acknowledged for the practical utility of the HER system. Using the imaging and analysis of exfoliated MoS_2 nanoplate as an example (Fig. 2), as illustrated in the scanning tunnelling microscopy (STM) result, the exfoliated MoS_2 nanoplate image provides a sufficiently clear image to graphically distinguish the morphological differences between the basal plane and the edge[16].

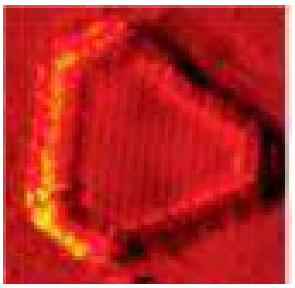

Figure 2: STM image of MoS2 nanoplate by exfoliation[16]

Moreover, the linear sweep voltammetry (LSV) measurement further indicates the significantly boosted HER performance after exfoliation with a milder Tafel slope of 94.31 mV/dec and lower onset potential, as shown in Fig. 3[17].

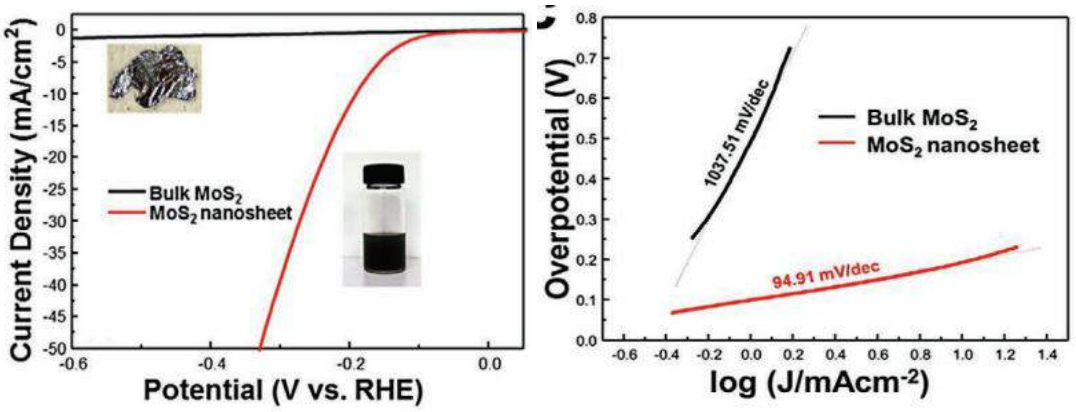

Figure 3: LSV curve (left) and the corresponding Tafel curve (right) between bulk MoS_2 and MoS_2 nanosheet to demonstrate the difference between both via chemical exfoliation methods[17]

4.2 Chemical formation of versatile nanostructured TMDs

Via chemical methodologies, various nanostructured morphologies can be well designed and constructed, like nanowires, nanosheets, nanoparticles, nanosized vertical alignments, mesoporous structures, and amorphous MoX_2[4, 10, 17, 18, 19]. These strategies strikingly reduce the overuse of raw materials under physical exfoliation. Zhang et al.[18] successfully generated high-density MoS_2 nanosheets vertically on polyaniline (PANI) nanowires, and synthesised 3D layered MoS_2/PANI composites. In this structure, PANI serves as architectural and electrical-conductive support for MoS_2, and the vertically aligned structure also exposes more edge active sites. MoS_2/PANI alignments deliver better HER catalytic performance than purely bulk states by maximising the most active edges[18].

Additionally, other useful morphological formations and characterisation techniques positively impact the overall analysis of versatile nanostructured TMDs. Binary TMDs, generated by incorporating another metallic atom into transition metal sulfides, suggest an extraordinarily enhanced activity compared with bulk materials.

Li et al.[19] fabricated $Mo_{(1-x)}$-W_x-S_2 composite as an ideal HER catalyst by a mild hydrothermal synthetic method. Here, the scanning electron microscopy (SEM) images (Fig. 4) indicate a well-defined spherical architecture with tensely attached nanopetals. Morphologically, it coincides with the pristine structure. Also, the transmission electron microscopy (TEM) image gives a higher-resolved picture of 2D stacked nanopetals. For further analysis of the composition, the exact formula of the composite is $Mo_{0.85}W_{0.15}S_2$ by X-ray photoelectron spectroscopy (XPS).

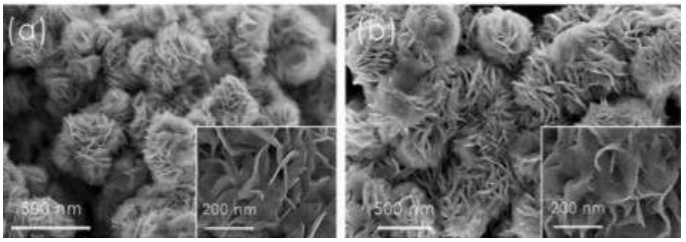

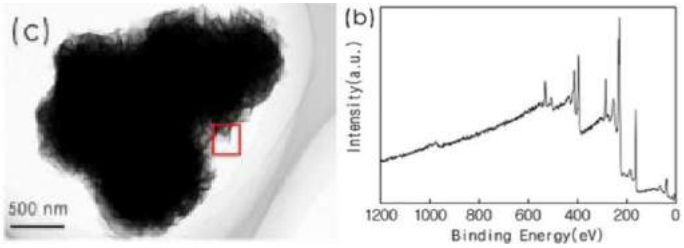

Figure 4: **(a)** SEM image of the pristine MoS_2; **(b)** SEM image of the $MoWS_2$ composite; **(c)** TEM image of the $MoWS_2$ composite; **(d)** overall XPS spectra of the composite[19]

V. REGULATING THE INTRINSIC ACTIVITY

5.1 Phase transition engineering

As one of the well-investigated TMD-related electrocatalytic materials, the activity of MoS_2 has been thoroughly understood. Due to its S-Mo-S layers in three different stacking ways, MoS_2 owns three possible prisms: 1T-, 2H-, and 3R-types[10]. 2H-MoS_2 is thermodynamically stable and exhibits the semiconducting characteristic, while the metastable 1T phase shows the metallic property. Consequently, the operable phase transition engineering from 2H to 1T makes a great difference to the electron conduction, driving the HER kinetics[8, 9, 12, 20]. Usually, 1T-types contribute to the boosted catalytic performance due to the higher density of active sites and metallic conductivity.

5.1.1 Ion intercalation

Lithium-ion intercalation is a common method for phase transformation. According to the test result of Lukowski et al.[20], the nanolayered 1T MoS_2 sheets reveal superior conductivity based on the AFM lithography in constant current mode. Similarly, from the electrochemical impedance spectroscopy (EIS) pattern, the charge transfer resistance of 2H sheets (232 Ω) sharply descends to 4 Ω with the transition, which also signifies a drastically rising electron conductivity (Fig. 5(b) and (c)). Likewise, Wang et al.[21] constructed a vertically arrayed electrode and precisely tuned the 2H-1T transition process by controlling the potentials, as Fig. 5(a) describes. More persuasively, their result explicitly reveals that the deeper Li+ discharge process leads to more spacing expansion of MoS_2 nanosheets and then boosts the HER kinetics.

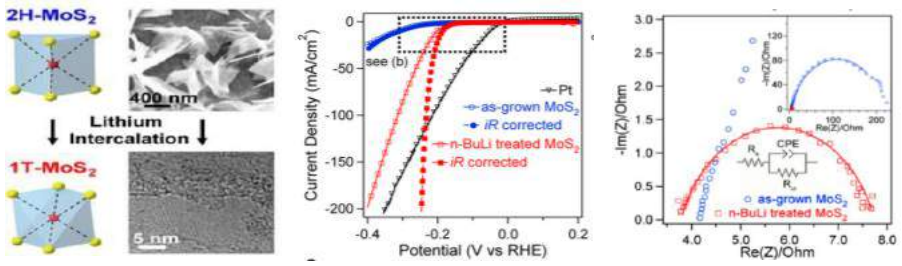

(a) (b) (c)

Figure 5: **(a)** Schematic diagram of the phase transition process from 2H- to 1T-MoS_2 induced by Li^+ intercalation; **(b)** current-potential curve depicting the electrocatalytic performance of Pt, 1T- (n-BuLi treated, in red) and 2H-MoS_2 nanosheets (as-grown, in blue) fabricated under different pretreatment conditions; **(c)** comparison of as-grown and n-BuLi treated MoS_2 in EIS spectrum[21]

Intercalation of extra ions has two roles in the phase transition process: 1) introducing new metal cations changes ΔG_H; 2) intercalation contributes to the electron injection into the nanosheets with the reduced charge and facilitates more catalytically active sites. With more intercalated ions, the intrinsic electronic structure can be efficiently and accurately modulated[22, 23].

5.1.2 Lattice strain

Besides ion intercalation, introducing strain also plays an indispensable role in the phase transition of TMDs. Tan et al.[24] synthesised a monolayered MoS_2 thin film on nanoporous Au substrate with a distorted surface. The surface distortion is demonstrated to form the lattice deformation and exert a strain-specific effect on the film: causing a measurable change in the S-Mo-S bond angle, thereby driving the localised 2H-1T phase transition. This approach can improve the state of density near the Fermi energy level by generating the corresponding stress, thereby leading to the localised 2H-1T phase transition and the loss of adsorption energy.

Recently, the combinations of atomic layer deposition (ALD) and electro-etching techniques were utilised to analyse the strain-affected HER performance. Specifically, Titanium Dioxide (TiO_2) was deposited on the plane of MoS_2 nanosheets by ALD, and the nanosheets were activated via an in-situ electrochemical method and then leached out to produce the strain. The testing result reveals a tremendous boost in the HER activity, as demonstrated in the LSV (Fig. 6(a)) and Tafel curves (Fig. 6(b)) respectively, and a positive correlation between the Tafel slope and the ALD cycle number (Fig. 6(c))[25].

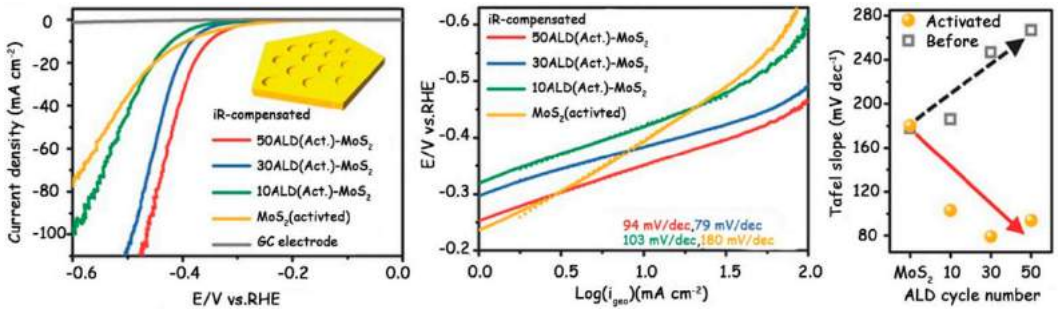

Figure 6: **(a)** iR-compensated LSV curves of MoS_2 (activated) and ALD(act.) MoS_2 at different scan cycles; **(b)** Tafel curves made based on (a); **(c)** graph showing the dependence of the Tafel slope and the ALD cycle number[25]

5.2 Defect engineering

Apart from increasing the density of electro-catalytically active edge sites, the basel plane possesses a larger surface area and proportion of potential sites for HER. Intentionally creating a new structural defects on the nanostructures of TMDs can tune the density of states more precisely and efficiently activate the intrinsically inert plane, then regulating the value of ΔG_H in H_2 generation[4, 8, 11-13]. The common form of the introduced defects in nanolayered TMDs contains point defects (vacancy, and atom impurity) and line defects (grain boundaries, GBs).

5.2.1 Introducing vacancies

Introducing the moderate number of S-vacancies can significantly enhance the HER activity by creating additionally new in-plane active sites.

Various techniques have been used to introduce more active vacancies, such as plasma treatment, chemical liquid exfoliation[26]. Compared with the LSV curves of pristine and plasma-treated MoS_2 with different time, with 15 minutes plasma treatment, MoS_2 has the optimal HER activity (Fig. 7), with the overpotential of 183 mV notably lower than that of pristine one (727 mV in Fig. 7(a))[26].

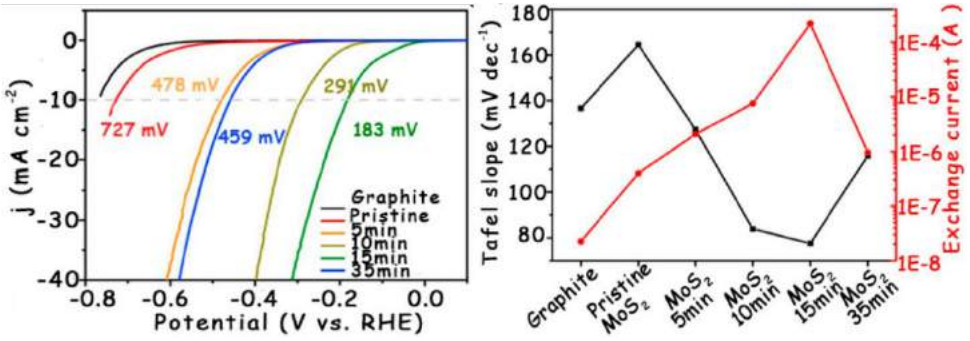

Figure 7: **(a)** polarisation curves of plasma-treated MoS_2 with various times; **(b)** the corresponding Tafel curve and exchange current curve[26]

Several computational discoveries based on synergic tuning of S atom vacancies and strain demonstrates the HER activity decreases with the lower concentration of S-vacancies[27]. The corresponding simulation shows that the best HER activity and kinetics should be under the optimal percentage of vacancies and elastic strains[28]. Hence, these results provide an instructive suggestion for the well-tuned HER system by enriching S-vacancies and applying strains simultaneously and appropriately.

5.2.2 Formation of high-density grain boundaries

Grain boundaries (GBs), also described as line defects, play a vital role in tuning the density of states and tailor the HER performance in atomically ultra-thin 2D TMD film. Due to hardship in controlling the structure and density of GBs, the connections of GBs and the HER activity attracts little attention. Theoretically, high-density GBs can create a new band near the Fermi level and narrow the energy gap, thereby modulating the HER spontaneous kinetics, which is similar to the role of vacancies[29].

He et al.[30] fabricated the wafer-size ultra-thin MoS_2 film (up to ~10^{12} cm^{-2}) via Au quan-tum-dot-assisted vapor-phase growth. Its exceedingly superior intrinsic electrocatalytic performance was comprehensively demonstrated by the onset potential (-25 mV) and the Tafel slope (54 mV/dec). The current density of the TMD nanograin film (about 1000 mA/cm^2) shows better performance than using CVD film bottom surface, with a single edge and GB assembled.

Most importantly, single Au is confirmed to have possibilities to contribute to the overall HER performance as a subsidiary part, but the main contributor is still the MoS_2 nanograin film[30].

VI. OPTIMISING THE ELECTRONIC STRUCTURE

6.1 Heteroatom doping

Doping heteroatoms is an efficient method to control the electronic structure and regulate the HER catalytic behaviour. Both metal sites and non-metal sites can be replaced to alter and tune the basic properties of TMD materials. Common categories of doped atoms can be divided into three parts: noble metals (Pt, Au, and Pd), non-noble metals (Co, Ni, Fe, Cu, V, and Zn) and non-metals (O, N, P, and B)[31]. The doped atoms can be located on edge or in the basal plane.

6.1.1 Metal doping

After the addition of metal dopants, due to the difference in the bond lengths and angles of Mo-S and X-S (X=metal) bonds, the in-plane distortion may generate the new electronic states and reduce the energy gap to alter the Gibbs Free Energy. Doping modification greatly optimises the adsoprtion of H atom and thereby, improve the in-plane intrinsic activity[8, 28, 32].

However, different metals may exert different influence on the HER kinetics and activity. Co/Ni-doped TMDs can remarkably reduce the value of ΔG_H and tune the local density of states[33]. Specifically, according to the DFT calculation, Co/Ni atoms result in a striking

decrease regarding the activation on the basel plane with a sharp change of ΔG_H from 1.5 eV to 0.15 eV under CV and LSV measurement. Conversely, Co/Ni modification causes little effect on the edge S sites.

6.1.2 Non-metal doping

Unlike the metal doping, nonmetal-doped TMDs do not only optimise the ΔG_H, but also replace the S sites to generate the lattice disorder and distortion because of the bond length and angle difference. This time, the modified electronic states will appear to modulate the intrinsic band structure and stimulate the electron conductivity as well as the H_2 generation reaction.

With an onset overpotential of 120 mV and a Tafel slope of 55 mV/dec, a boosted HER performance got a thorough verification by incorporating oxygen atoms, which reveals the tuning in both covalent and conduction band of TMDs[30].

6.2 Surface functionalisation with organic molecules

The coupling system can decrease the gap width and facilitate the charge transfer process by altering the band structure and TMDs-based hydrogen adsorption kinetics. Organic ligands with specific functional groups are the most common category as an electron donor[34, 35]. As the catalytically organic ligand, the only one for HER enhancement is thiobarbituric acid (TBA) among versatile functional groups. As mentioned in Presolski et al.[35], the main reasons are 1T-phase metallic properties, the poorly basic and wettable environment on the surface. Also, the calculation result shows a highly boosted activity with low or high coverage of TBA molecules, where 50% of the TBA contributes to the maximally superior performance.

However, the tedious processing and time consuming procedures may hinder the main focus of this functionalised coupling system.

VII. SUMMARY AND PERSPECTIVES

We comprehensively summarised the modification strategies and the state-of-the-art advances of HER electrocatalysts based on 2D TMDs. Following the composition characterisation construction guideline, we offered three methodologies for HER enhancement: 1) to increase the active sites; These strategies can boost HER performance individually or in a synergic way to highlight their 2) to improve the intrinsic conductivity and activity; 3) to optimise the electronic structure. roles in structural design and electronic modulation. Both theoretical and experimental findings play vital roles in more insight into TMDs-related HER system, as comprehensively summarised in Fig. 8.

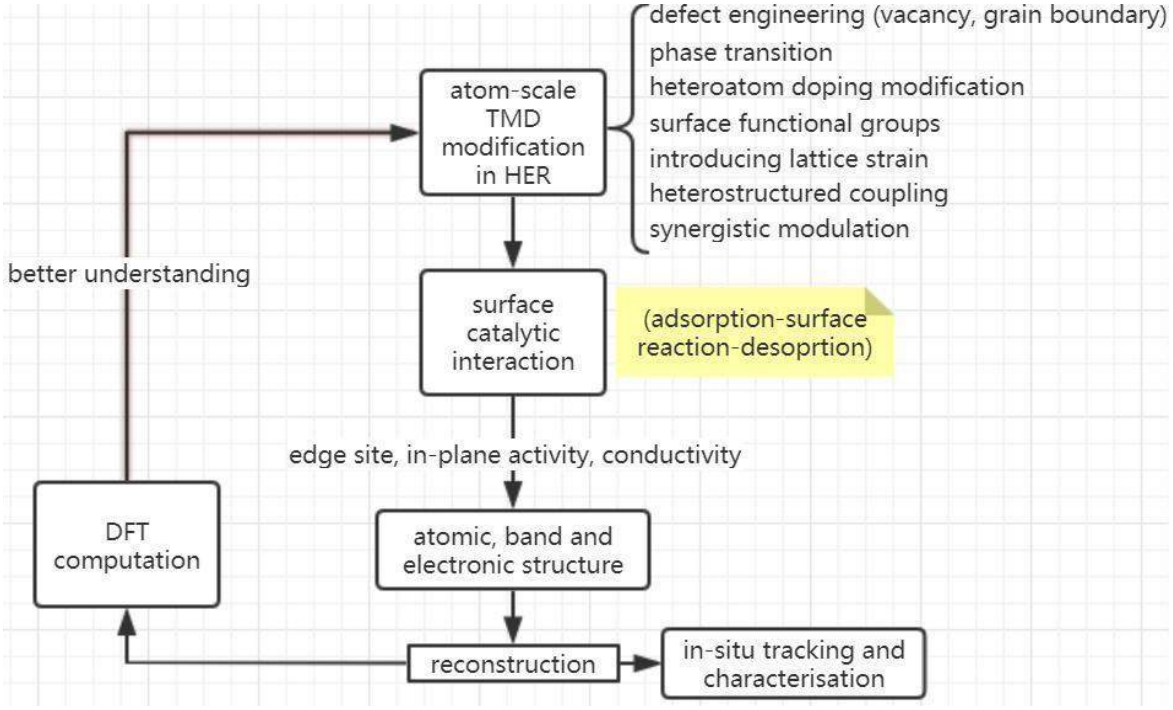

Figure 8: schematic principles of the optimal design and modulation of TMDs-based HER electrocatalysts based on the composition-characterisation-construction guideline

However, there is still a long way to go before the broad application of TMDs based catalysts in water electrocatalysis:

1. Regarding the nano-level synthesis of TMDs, there is a lack of systematic theoretical guidance and well-tuned fabrication methods;
2. The correlations in HER catalytic activity and nanostructures of TMDs is unclear;
3. More intelligent algorithms are urgently needed to narrow the gap between experimental and simulated results.
4. Lastly, the long-term stability of catalysts should be highlighted. The large-scale application needs electrocatalysts with extraordinary long-term stability and durability.

Overall, the 2D TMDs exhibit great potential to replace the noble-metal HER electrocatalysts (Pt) for efficient water electrochemical splitting. By the rational optimal design of TMDs. It is possible to achieve a wide-ranging commercial application.

REFERENCES

1. Turner, J. A. Sustainable Hydrogen Production. Science 2004, 305, 972-974.
2. Tabassum, H.; Mahmood, A.; Zhu, B.; Liang, Z.; Zhong, R.; Guo, S.; Zou, R. Recent Advances in Confining Metal-Based Nanoparticles into Carbon Nanotubes for Electrochemical Energy Conversion and Storage Devices. Energy Environ. Sci. 2019, 12, 2924-2956.
3. Liu, Y.; Wu, J.; Hackenberg, K. P.; Zhang, J.; Wang, Y. M.; Yang, Y.; Keyshar, K.; Gu, J.; Ogitsu, T.; Vajtai, R. Self-Optimizing, Highly Surface-Active Layered Metal Dichalcogenide Catalysts for Hydrogen Evolution. Nat. Energy 2017, 2, 17127.
4. Zhang, J.; Wang, T.; Liu, P.; Liu, S.; Dong, R.; Zhuang, X.; Chen, M.; Feng X. Engineering Water Dissociation Sites in MoS_2 Nanosheets for Accelerated Electrocatalytic Hydrogen Production. Energy Environ. Sci. 2016, 9, 2789-2793.

5. Zou, X.; Zhang, Y. Noble Metal-Free Hydrogen Evolution Catalysts for Water Splitting. Chem. Soc. Rev. 2015, 44, 5148-5180.
6. Li, T.; Li, S.; Liu, Q.; Yin, J.; Sun, D.; Zhang, M.; Xu, L.; Tang, Y.; Zhang, Y. Immobilization of Ni_3Co Nanoparticles into N-Doped Carbon Nanotube/Nanofiber Integrated Hierarchically Branched Architectures toward Efficient Overall Water Splitting. Adv. Sci. 2020, 7, 1902371.
7. Thanh, T. D.; Chuong, N. D.; Hien, H. V.; Kshetri, T.; Tuan, L. H.; Kim, N. H.; Lee, J. H. Recent Advances in Two-Dimensional Transition Metal Dichalcogenides-Graphene Heterostructured Materials for Electrochemical Applications. Prog. Mater. Sci. 2018, 96, 51-85.
8. Cheng, C. -C.; Lu, A. -Y.; Tseng, C. -C.; Yang, X.; Hedhili, M. N.; Chen, M.-C.; Wei, K. -H.; Li, L. -J. Activating Basal-Plane Catalytic Activity of Two-Dimensional MoS_2 Monolayer with Rem- ote Hydrogen Plasma. Nano Energy 2016, 30, 846-852.
9. Meng, C.; Chen, X.; Gao, Y.; Zhao, Q.; Kong, D.; Lin, M.; Chen, X.; Li, Y.; Zhou, Y. Recent Modification Strategies of MoS_2 for Enhanced Electrocatalytic Hydrogen Evolution. Molecules 2020, 25, 1136.
10. Zhu, J.; Hu, L.; Zhao, P.; Lee, L. Y. S.; Wong, K. -Y. Recent Advances in Electrocatalytic Hydrogen Evolution Using Nanoparticles. Chem. Rev. 2020, 120, 851-918.
11. Morales-Guio, C. G.; Stern, L. -A.; Hu, X. L. Nanostructured Hydrotreating Catalysts for Electrochemical Hydrogen Evolution. Chem. Soc. Rev. 2014, 43, 6555-6569.
12. Garlyyev, B.; Fichtner, J.; Piqué, O.; Schneider, O.; Bandarenka, A. S.; Calle-Vallejo, F. Revealing the Nature of Active Sites in Electrocatalysis. Chem. Sci. 2019, 10, 8060-8075.
13. Tributsch, H.; Bennett, J. C. Electrochemistry and Photochemistry of MoS_2 Layer Crystals. 1. J. Electroanal. Chem. 1977, 81, 97-111.
14. Hinnemann, B.; Moses, P. G.; Bonde, J.; Jorgensen, K. P.; Nielsen, J. H.; Horch, S.; Chorkendorff, I.; Norskov, J. K. Biomimetic Hydrogen Evolution: MoS_2 Nanoparticles as Catalyst for Hydrogen Evolution. J. Am. Chem. Soc. 2005, 127, 5308–5309.
15. Jaramillo, T. F.; Jorgensen, K. P.; Bonde, J.; Nielsen, J. H.; Horch, S.; Chorkendorff, I. Identification of Active Edge Sites for Electrochemical H_2 Evolution from MoS_2 Nanocatalysts. Science 2007, 317, 100-102.
16. Yin, Z.; Li, H.; Li, H.; Jiang, L.; Shi, Y.; Sun, Y.; Lu, G.; Zhang, Q.; Chen, X.; Zhang, H. Single-Layer MoS_2 Transistors. ACS Nano 2012, 6, 74-80.
17. Nguyen, T. P.; Choi, S.; Jeon, J. -M.; Kwon, K. C.; Jang, H. W.; Kim, S. Y. Transition Metal Disulfide Nanosheets Synthesized by Facile Sonication Method for the Hydrogen Evolution Reaction. J. Phys. Chem. C 2016, 120, 3929-3935.
18. Zhang, N.; Ma, W.; Wu, T.; Wang, H.; Han, D.; Niu, L. Edge-Rich MoS_2 Naonosheets Rooting into Polyaniline Nanofibers as Effective Catalyst for Electrochemical Hydrogen Evolution. Electrochim Acta 2015, 180, 155-163.
19. Li, H.; Yu, K.; Tang, Z.; Zhu, Z. Experimental and First-Principles Investigation of $MoWS_2$ with High Hydrogen Evolution Performance. ACS Appl. Mater. Interfaces 2016, 8, 29442-29451.
20. Zhou, S.; Han, J.; Sun, J.; Srolovitz, D. J. MoS_2 Edges and Heterophase Interfaces: Energy, Structure and Phase Engineering. 2D Mater. 2017, 4, 025080.
21. Lukowski, M. A.; Daniel, A. S.; Meng, F.; Forticaux, A.; Li, L.; Jin, S. Enhanced Hydrogen Evolution Catalysis from Chemically Exfoliated Metallic MoS_2 Nanosheets. J. Am. Chem. Soc. 2013, 135, 10274-10277.
22. Attanayake, N. H.; Thenuwara, A. C.; Patra, A.; Aulin, Y. V.; Tran, T. M.; Chakraborty, H.; Borguet, E.; Klein, M. L.; Perdew, J. P.; Strongin, D. R. Effect of Intercalated Metals on the Electrocatalytic Activity of 1T-MoS_2 for the Hydrogen Evolution Reaction. ACS Energy Lett .2017 ,3 ,7-13 .
23. Chen, Y. C.; Lu, A.; Lu, P.; Yang, X.; Jiang, C.; Mariano, M.; Kaehr, B.; Lin, O.; Taylor, A.; Sharp, D.; Li, L.; Chou, S. S.; Tung, V.

Structurally Deformed MoS_2 for Electrochemically Stable, Thermally Resistant, and Highly EfficientHydrogen Evolution Reaction. Adv. Mater. 2017, 29, 1703863.
24. Tan, Y.; Liu, P.; Chen, L.; Cong, W.; Ito, Y.; Han, J.; Guo, X.; Tang, Z.; Fujita, T.; Hirata, A.; Chen M. W. Monolayer MoS_2 Films Supported by 3D Nanoporous Metals for High-Efficiency Electrocatalytic Hydrogen Production. Adv. Mater. 2014, 26, 8023-8028.
25. Kim, Y.; Jackson, D. H. K.; Lee, D.; Choi, M.; Kim, T. -W.; Jeong, S. -Y.; Chae, H. -J.; Kim, H. W.; Park, N.; Chang, H.; Kuech, T. F.; Kim, H. J. In Situ Electrochemical Activation of Atomic Layer Deposition Coated MoS_2 Basal Planes for Efficient Hydrogen Evolution Reaction. Adv. Funct. Mater. 2017, 27, 1701825.
26. Cheng, C. -C.; Lu, A. -Y.; Tseng, C. -C.; Yang, X.; Hedhili, M. N.; Chen, M. -C.; Wei, K. -H.; Li, L. -J. Activating Basal-Plane Catalytic Activity of Two-Dimensional MoS_2 Monolayer with Remote Hydrogen Plasma. Nano Energy 2016, 30, 846–852.
27. Lin, S. -H.;Kuo, J. -L. Activating and Tuning Basal Planes of MoO_2, MoS_2, and $MoSe_2$ for Hydrogen Evolution Reaction Phys. Chem. Chem. Phys. 2015, 17, 29305-29310.
28. Gao, D.; Xia, B.; Zhu, C.; Du, Y.; Xi, P.; Xue, D.; Ding, J.; Wang, J. Activation of the $MoSe_2$ Basal Plane and Se-Edge by B Doping for Enhanced Hydrogen Evolution. J. Mater. Chem. A 2018, 6, 510-515.
29. Son, D. -Y.; Lee, J. -W.; Choi, Y. J.; Jang, I. -H.; Lee, S.; Yoo, P. J.; Shin, H.; Ahn, N.; Choi, M.; Kim, D.; Park, N. -G. Self-Formed Grain Boundary Healing Layer for Highly Efficient CH_3-NH_3-PbI_3 Perovskite Solar Cells. Nat. Energy 2016, 1, 16081.
30. He, Y.; Tang, P.; Hu, Z.; He, Q.; Zhu, C.; Wang, L.; Zeng, Q.; Golani, P.; Gao, G.; Fu, W.; et al. Engineering Grain Boundaries at the 2D Limit for the Hydrogen Evolution Reaction. Nat. Commun. 2020, 11, 1-12.
31. Bonde, J.; Moses, P. G.; Jaramillo, T. F.; Nørskov, J. K.; Chorkendorff, I. Hydrogen Evolution on Nano-Particulate Transition Metal Sulfides. Faraday Discuss. 2009, 140, 219-231.
32. Zhang, J.; Xu, X.; Yang, L.; Cheng, D.; Cao, D. Single-Atom Ru Doping Induced Phase Transition of MoS_2 and S Vacancy for Hydrogen Evolution Reaction. Small Methods 2019, 3, 1900653.
33. Zhang, H.; Yu, L.; Chen, T.; Zhou, W.; Lou, X. W. D. Surface Modulation of Hierarchical MoS_2 Nanosheets by Ni Single Atoms for Enhanced Electrocatalytic Hydrogen Evolution. Adv. Funct. Mater. 2018, 28, 1807086.
34. Tvrdy, K.; Frantsuzov, P. A.; Kamat, P. V. Photoinduced Electron Transfer from Semiconductor Quantum Dots to Metal Oxide Nanoparticles. PNAS 2011, 108, 29-34.
35. Presolski, S.; Wang, L.; Loo, A. H.; Ambrosi, A.; Lazar, P.; Ranc, V.; Otyepka, M.; Zboril, R.; Tomanec, O.; Ugolotti, J.; et al. Functional Nanosheet Synthons by Covalent Modification of Transition-Metal Dichalcogenides. Chem. Mater. 2017, 29, 2066-2073.

This page is intentionally left blank

Water Sorption Isotherms of Sorghum Grains (*sorghum Bicolor* L. Moench) Under Different Temperatures and Water Activities

Eman Abdu Abdalla, Adam Bush Adam, *Saher Gaafer Ahmed & Abdelmoneim Elamin Mohamed*

University of Bakht El Ruda, Elddium

ABSTRACT

In the semi arid conditions of Sudan, the determination of moisture sorption isotherms at different temperatures and water activities to establish the correctly storage conditions for crops grains is highly needed. The objective of this study was to determine the moisture sorption isotherms of two local varieties of sorghum (Sorghum bicolor L Moench.) namely; Tabat and Wad Ahmed at various temperatures and water activities. The study was conducted at the Department of Agricultural Engineering, University of Khartoum and the Department of Grains Technology, Food Research and Processing Center, Shambat, Sudan during the period from December 2006 to December 2008.

Keywords: water activity, water sorption isotherms; sorghum.

Classification: FOR Code: 291899p

Language: English

London Journals Press

LJP Copyright ID: 925652
Print ISSN: 2631-8490
Online ISSN: 2631-8504

London Journal of Research in Science: Natural and Formal

Volume 21 | Issue 3 | Compilation 1.0

Water Sorption Isotherms of Sorghum Grains (*sorghum Bicolor* L. Moench) Under Different Temperatures and Water Activities

Eman Abdu Abdalla[α], Adam Bush Adam[σ*], Saher Gaafer Ahmed[ρ] & Abdelmoneim Elamin Mohamed[ω]

ABSTRACT

In the semi arid conditions of Sudan, the determination of moisture sorption isotherms at different temperatures and water activities to establish the correctly storage conditions for crops grains is highly needed. The objective of this study was to determine the moisture sorption isotherms of two local varieties of sorghum (Sorghum bicolor L Moench.) namely; Tabat and Wad Ahmed at various temperatures and water activities. The study was conducted at the Department of Agricultural Engineering, University of Khartoum and the Department of Grains Technology, Food Research and Processing Center, Shambat, Sudan during the period from December 2006 to December 2008. Water sorption isotherms were determined using standard static gravimetric method at temperatures 25°C; 35°C and 45°C over a range of water activities from 0.112 to 0.865. The water activities were maintained using saturated salt solutions inside air-tight glass desiccators, while incubators were used to maintain a constant temperature. The results showed that, there is a highly significant (P ≤ 0.01) effect of water activity nested within temperature and also for the interaction between water activity nested within temperature and cultivars. Wad Ahmed cultivar gave the highest values of adsorption (13.633%db) and desorption (15.665%db) equilibrium as compared to Tabat cultivar (13.615%db and 15.410%db, respectively) at the same temperature and water activities. Increasing temperature from 25°C to 45°C decreased the sorption isotherms at a constant water activity, while increasing water activities from 0.112 to 0.865 increased the sorption isotherms for both adsorption and desorption equilibrium at a constant temperature. It is concluded that, moisture sorption isotherms of sorghum grains play important roles in such technological processes as drying, handling, packaging, storage, mixing and other processes that requires the prediction of food stability, glass transition and estimation of drying time and texture and prevention of deteriorative reactions.

Keywords: water activity, water sorption isotherms; sorghum.

Author α: Department of Agricultural Engineering, Faculty of Agricultural &Natural Rescores, University of Bakht El Ruda, Elddium, Sudan.
σ: Department of Agricultural Engineering, Faculty of Natural Rescores and Environmental Studies, University of Alsalam, Alfula, Sudan.
ρ ω: Department of Agricultural Engineering, Faculty of Agriculture, University of Khartoum, Shambat, Sudan.

I. INTRODUCTION

Sorghum (*Sorghum bicolor* (L.) Moench) is a major cereal cultivated as food and feed in the semi arid regions of the world. It plays a crucial role in the world food economy as it contributes to rural household food security. It feeds millions of people on a daily basis in the developing countries, providing dietary starch and proteins, some vitamins and minerals phytochemicals with substantiated health benefits (Taylor and Duodu, 2017; Adebo *et al*., 2018). In Sudan, sorghum grain is the most important staple cereal food crop for human nutrition as they are the major sources of nutrients, proteins and calories for populations. Sorghum grain storage including above ground and underground facilities. Both types include

London Journal of Research in Science: Natural and Formal

traditional and modern storage facilities. However, large amounts of grain are lost during post harvest operations such as threshing, cleaning, storing and transportation. Evidently, this is due to the poor traditional harvesting and storage methods as well as the inadequate threshing tools. Grain losses in the traditional stores can reach 50%, they range between 5% and 13% for modern storage facilities; 6%in the underground pits and only 1% in silos (Abdalla *et al.*, 2002). Therefore, the knowledge of moisture sorption isotherms of cereal and oilseed grains are so essential in order to establish storage condition since they give information about the humidity-water activity (a_w) relation at given temperature, to prevent deterioration during storage (Bianco *et al.*, 2007). The sorption of moisture by the product from the atmosphere and the atmosphere from the product will occur during storage and packaging. The moisture sorption isotherm of food graphically relates its equilibrium moisture content in either desorption or adsorption, to the water activity (aw) at a definite temperature. These isotherms are extremely important quantitative measures in food preservation, storage, packaging and drying (Chen, 2000, Arslan Togrul, 2005 and Medeiros *et al.*, 2006). Equilibrium moisture content for the adsorption and desorption processes does not have the same values. Grain that is losing moisture to the air i.e. desorption or drying, has a higher equilibrium moisture content than if the same grain being initially at lower moisture content began adsorbing moisture from air at the same relative humidity. The equilibrium moisture content for desorption is higher than for adsorption at a particular water activity. Raji and Ojediran (2011) determined moisture sorption isotherms of millets at temperature range of 30–70◦C and water activity range of 0.07–0.98 using the static gravimetric method. His result revealed that, sorption isotherms of millet decreased with increasing temperature. Water activity revealed the material's interaction with environmental conditions to determine the amount of moisture that can be lost or gained, or the relative closeness of any given moisture content to one that represents product stability in storage. The relationship between the water activity (aw) and moisture content of a material at a given temperature is called the moisture sorption isotherm which divided into three zones; Zone I (aw < 0.25) represents the monolayer water, which is strongly associated with the food material, unable to freeze and not easily removed by drying. Zone II (0.25 < aw < 0.75) represents the water that is adsorbed or absorbed in multi layers within foods and solutions of soluble components. Zone III (aw > 0.75) represents the "free" water, which is available for microbial growth and enzymatic activity and freezable and easily removed by drying (Fennma, 1996). Arabhosseini *et al.* (2010) and Chico-Santamarta *et al.* (2011) stated that, water activity between 0.6 and 0.7 represents the maximum allowable level to limit microbial degradation in aerobic storage. Bonner and Kenney (2013) reported that, water activity decreased with increasing temperatures. In Sudan, no effort has been reported on determining the moisture sorption isotherms properties of Sorghum (Sorghum. *bicolor* L. Moench) at various temperatures to establish the storage conditions. Therefore the objective of this study was to evaluate the moisture sorption isotherms of Sorghum (Sorghum. *bicolor* L. Moench) at various temperatures and water activities

II. MATERIALS AND METHODS

2.1 Experimental work

The experimental work was carried out at the Department of Agricultural Engineering, University of Khartoum and the Department of Grains Technology, Food Research and Processing Center, Shambat, Sudan during the period from December 2006 to December 2008. For the study purpose, two local sorghum grains varieties namely, Tabat and Wad Ahmed (Plate 1 and 2) were obtained from Sorghum Research Programme, Agricultural Research Corporation, Wad Medani, Gezira State, Sudan.

2.2 Equipments

The following equipment was used in the experiments.

1. A sensitive balance: model AB54-S, Mettlre Toledo make and made in Switzerland, with

an accuracy of ±0.001 g was used for weighing the samples in the different experiments.

2. An air-oven: model KAT-NR 28452 Elektro-Helios makes and made in Sweden was used for the determination of the moisture content (m.c.).
3. Two incubators: model Gallenkamp make and made in England both with temperature range of -10°C to 50°C (Plate 3.3) were used for determination of sorption isotherms of samples.
4. A hardness tester: model No.174886make and made by Seiskusho LTD – Japan was used to measure grain hardness.
5. A shaker apparatus: model KL. 2 No. 490 Edumund Bühler make and made in Germany was used for preparation of sorghum samples for desorption test. .
6. A venire caliper: was used for measuring the size of grains.
7. A refrigerator: model Sanyo-Freezer makes and made in Germany was used for storing sorghum samples.
8. A hectoliter: was used for determination of test weight of grain sample.
9. Crucible containers: were used to determine ash contents of grain sample.
10. A thermometer: was used to measure the temperatures.
11. Aluminum dishes or containers: were used for determination of moisture contents of grain sample.
12. Graduated measuring cylinders: with a volume of 100 ml were used for measuring the volume of distilled water.
13. A small micro-Kjeldhl flask with volume of 100 ml was used for determination of protein contents of grains sample.
14. A glass rod: was used to stir the saturated salt solutions.
15. A hair hygrometer: was used to check the attained air relative humidities of the saturated solutions.
16. Glass desiccators: in which samples of sorghum were tested for equilibrium moisture content (EMC.) determination
17. Conical flasks: each with volume of 250 ml for the preparation of the saturated salt solutions.

III. ADSORPTION AND DESORPTION ISOTHERMS AND EQUILIBRIUM MOISTURE CONTENT (EMC) DETERMINATION

For adsorption and desorption isotherms of the samples the standard static gravimetric method as stated by Wolf *et al.*, (1985) was used. For adsorption isotherms the samples were dried to (3.03%) dry basis, of moisture content, by using an air oven (KAT-NR 28452 Elektro-Helios, Sweden) with air circulation and the air temperature was adjusted at 40°C to achieve the final moisture content for adsorption. The final weight that gave the dried samples was determined by using the equation (1) as described by Gough (1983). A saturated salt solution of potassium chromate (K_2CrO_4) maintaining water activity of 0.865 was prepared at a temperature of 25°C ± 1.0°C and was used to determine the range of the expected values for desorption equilibrium moisture content of grain samples. Three samples each of 500 g in weight were taken from the dried grains of each cultivar and placed in Kilner air tight jars. The amount of distilled water added to each jar to condition the grains so as to obtain the intended moisture content range was determined using the equation (2) as reported by Gough (1983). The jars were placed onto a shaker device (Edumund Bühler, KL. 2 No. 490, Germany) for preparation of the samples for desorption test of moisture content of 32.02% dry basis. The shaking was done over a period of three days, four times a day, for 45 minutes following the procedure reported by Ismail (1994). All the jars were emptied and the samples wrapped in aluminum foil and put inside polyethylene bags and stored in the refrigerator until they were used for EMC determination. The wetted sorghum samples were allowed to equilibrate for 6 h in the room condition before being used.

$$B = \frac{A\,(100-a)}{(100-b)} \quad \text{..... (1)}$$

$$Q = \frac{A\,(b-a)}{(100-b)} \quad \text{..... ..... (2)}$$

Where:

B = Final weight of sample after drying kg.

Q = Weight of water to be added kg.

A = Initial weight of sample before drying kg.

a = Initial moisture content of sample (percent wet basis).

b = Desired final moisture content of sample (percent wet basis).

The standard static gravimetric method as stated by Wolf *et al.*, (1985) was used for determining the equilibrium moisture content data for both adsorption and desorption isotherms. Triplicates of pre-conditioned samples (10g ±0.001g each for desorption and 5g ±0.001g each for adsorption) were placed on circular plastic Petri dishes placed on a plastic platform inside the glass desiccators. Six saturated salt solutions, which were used to maintain the constant water activities, are shown in Table 1. The salt solutions and the samples were put in the desiccators which were placed inside incubators (Gallenkamp, temperature range of -10°C to 50°C, England) with, adjusted at 25°C; 35°C and 45°C±1.0°C. The samples were weighed daily using an electronic sensitive balance until a constant weight with obtained from three successive readings was a difference of ± 0.001g. The final moisture content of the samples, after attaining equilibrium was determined according to the standard method of the Association of Official Analytical Chemists (AOAC, 1990). In this method, well-mixed triplicate of grain samples each of an initial weight of about 2 ± 0.001 g were dried in an air-oven set at 105±1.0°C for 24 hours. The moisture content of the samples determined on percent dry basis at this stage was EMC. All the experiments were carried in triplicates and the average value at each temperature and water activity was determined.

3.1 Water activity (a_w) determination

Water activity (a_w) can be given by the following equation mentioned by McLaughin and Magee (1998):

$$a_w = \frac{P_f}{P_o} = \frac{ERH}{100} \quad (3)$$

Where:

aw = Water activity decimal
Pf = Vapour pressure of water in the food Nm-2.
Po = Vapour pressure of pure water at the same temperature Nm-2
ERH = Equilibrium relative humidity %

Table 1: Water activity (a_w) values of the saturated salt solutions at three temperatures, 25°C, 35°C and 45°C.

Salt chemical formula	Water activity (a_w)		
	25°C	35°C	45°C
LiCL	0.112	0.112	0.113
$KC_2H_3O_2$	0.227	0.184	0.195
K_2CO_3	0.438	0.435	0.432
Na NO_2	0.643	0.633	0.605
NaCl	0.748	0.756	0.745
K_2CrO_4	0.865	0.863	0.846

Source: Kalemullah and Kaillappan (2004)

IV. EXPERIMENTAL DESIGN

A factorial experimental design of three factors namely; two varieties, three temperature levels and six levels of water activity being nested within temperature. Data were analyzed following the method described for a completely randomized design. Statistical tools such as ANOVA and DMRT were used to analyze the experimental data.

Plate 1: Tabat sorghum cultivar

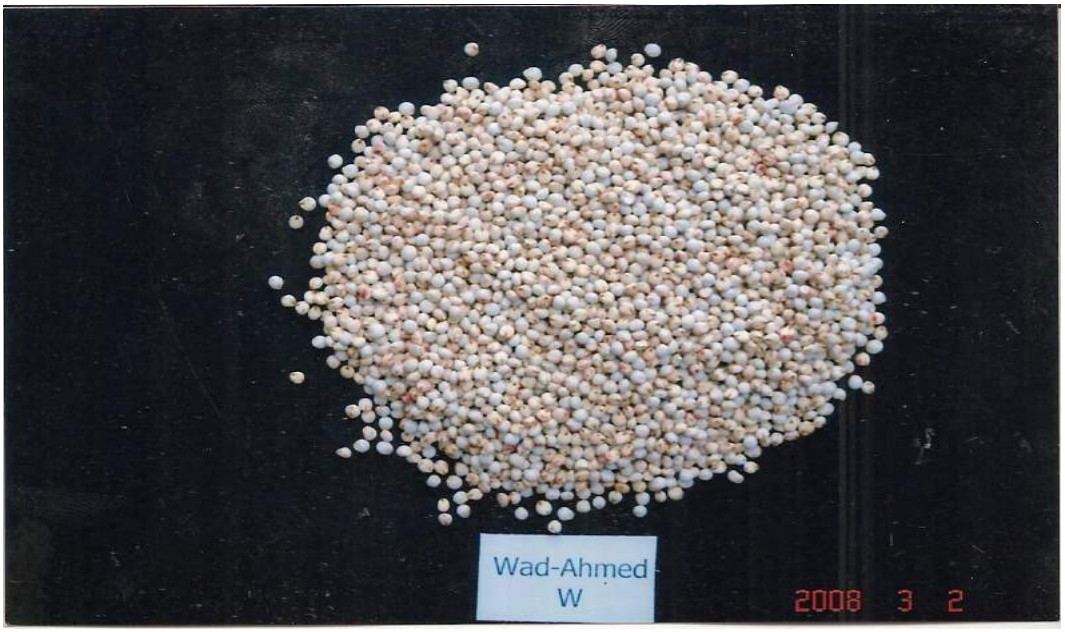

Plate 2: Wad Ahmed sorghum cultivar

V. RESULTS AND DISCUSSION

Moisture sorption characteristics of agricultural and food products play important roles in such technological processes as drying, handling, packaging, storage, mixing, freeze-drying and other processes that requires the prediction of food stability, shelf life, glass transition and estimation of drying time and texture and prevention of deteriorative reactions.

The relationship between the adsorption moisture sorption isotherms and the two local sorghum cultivars, temperature and water activity was

presented in Table 1 and Fig. 1 and 2. Equilibrium moisture content for the adsorption and desorption processes does not have the same values. Statistical analysis showed that, there were a highly significant effect ($P \leq 0.05$) between moisture sorption isotherms and two local varieties and also for the interaction between water activity nested within temperature and cultivars. It is clear that, the adsorption means values for Wad Ahmed cultivar is greater than Tabat cultivar. On the other hand, increasing temperature from 25°C to 45°C decreased the equilibrium moisture content for a constant water activity. So the change in adsorption value among the temperature differs with the change in sorghum cultivars, the highest values are obtained for both cultivars at 25°C. The adsorption value for each cultivar was increasing with the increases in water activity nested within temperature. The highest values were obtained under the highest water activity at 25°C for Wad Ahmed cultivar compared to Tabat cultivar. The results were in conformity with the results obtained by Raji and Ojediran (2011) who determined moisture sorption isotherms of millets at temperature range of 30–70◦C and water activity range of 0.07–0.98 using the static gravimetric method. His result revealed that, sorption isotherms of millet decreased with increasing temperature.

The water activity of foods at higher temperatures plays a major role during drying and storage of dry products. The changing in water activity of food ingredients and effective diffusivity to control moisture migration in multi domain foods, when temperature changes occur is highly difference. Increasing water activity from 0.112 to 0.865 increased the equilibrium moisture content for both the adsorption and desorption isotherms at a constant temperature. The relationship between equilibrium moisture content and water activity at various temperatures was found to decrease with increasing temperatures. The results confirmed that, water activity decreased with increasing temperatures as mentioned by Bonner and Kenney (2013). Therefore, the results were in agreement with the results obtained by Arabhosseini *et al.* (2010) and Chico-Santamarta *et al.* (2011) who mentioned that, water activity between 0.6 and 0.7 represents the maximum allowable level to limit microbial degradation in aerobic storage.

Table 2 and Fig. 3 and 4 showed that, the equilibrium moisture content for desorption is higher than for adsorption at a particular water activity. The desorption value for each cultivar increased with the increase in water activity nested within temperature. The highest desorption values was obtained for the highest water activity at 25°C. The change in desorption value among the temperature differs with the change in sorghum cultivars, the highest value of desorption was recorded under Wad Ahmed cultivar as compared to Tabat cultivar at 25°C. These results were in agreement with result obtained by Togrul and Togrul and Arslan (2006) who reported that, many food deterioration reactions and the growth of important microorganisms such as fungi depend on the water activity of the food, and water activity is thus an important variable to produce food stability.

Table 1: Mean values of adsorption equilibrium moisture content (% d.b) for sorghum grain cultivars at different temperatures and water activities

Temperature (°C)	Water activity (decimal)	Variety (% d.b)		Mean
		Tabat	Wad Ahmed	
25	0.112	6.799^{h}	7.198^{g}	6.999^{p}
	0.227	10.921^{f}	11.024^{f}	10.977^{k}
	0.438	11.728^{d}	11.310^{e}	11.747^{j}
	0.643	15.559^{c}	15.655^{c}	15.607^{g}
	0.748	16.783^{b}	16.874^{b}	16.829^{d}

	0.865	19.785[a]	19.735[a]	19.747[a]
	Mean	13.592[a]	13.633[a]	13.615[a]
35	0.112	6.288[m]	6.458[k]	6.373[q]
	0.184	8.636[k]	8.889[i]	8.763[n]
	0.435	9.841[hi]	9.945[g]	9.893[l]
	0.633	13.429[g]	14.859[e]	14.144[h]
	0.756	16.198[e]	16.328[c]	16.264[e]
	0.863	18.861[b]	18.977[b]	18.919[b]
	Mean	12.209[b]	12.577[b]	12.396[b]
45	0.113	5.208[j]	5.317[j]	5.263[r]
	0.195	7.890[i]	8.566[h]	8.228[o]
	0.432	9.032[g]	9.268[f]	9.150[m]
	0.605	12.732[c]	13.355[c]	13.044[i]
	0.745	15.650[c]	15.932[d]	15.791[f]
	0.846	18.847[a]	18.742[a]	18.794[c]
	Mean	11.560[d]	11.863[c]	11.712[c]
Means of variety		12.453[a]	12.699[a]	

Means with the same letter are not significantly different from each other, according to Duncan's Multiple Range Test (DMRT).

Table 2: Mean values of desorption equilibrium moisture content (% d.b) for sorghum grain cultivar at different temperatures and water activities

Temperature (°C)	Water activity (decimal)	Variety (% d.b)		Mean
		Tabat	Wad Ahmed	
25	0.112	6.799[h]	7.198[g]	6.999[p]
	0.227	10.921[f]	11.024[f]	10.977[k]
	0.438	11.728[d]	11.310[e]	11.747[j]
	0.643	15.559[c]	15.655[c]	15.607[g]
	0.748	16.783[b]	16.874[b]	16.829[d]
	0.865	19.785[a]	19.735[a]	19.747[a]
	Mean	13.592[a]	13.633[a]	13.615[a]
35	0.112	6.288[m]	6.458[k]	6.373[q]
	0.184	8.636[k]	8.889[i]	8.763[n]
	0.435	9.841[hi]	9.945[g]	9.893[l]
	0.633	13.429[g]	14.859[e]	14.144[h]
	0.756	16.198[e]	16.328[c]	16.264[e]
	0.863	18.861[b]	18.977[b]	18.919[b]
	Mean	12.209[b]	12.577[b]	12.396[b]
45	0.113	5.208[j]	5.317[j]	5.263[r]
	0.195	7.890[i]	8.566[h]	8.228[o]
	0.432	9.032[g]	9.268[f]	9.150[m]
	0.605	12.732[c]	13.355[c]	13.044[i]
	0.745	15.650[c]	15.932[d]	15.791[f]
	0.846	18.847[a]	18.742[a]	18.794[c]
	Mean	11.560[d]	11.863[c]	11.712[c]
Means of variety		12.453[a]	12.699[a]	

Means with the same letter are not significantly different from each other, according to Duncan's Multiple Range Test (DMRT).

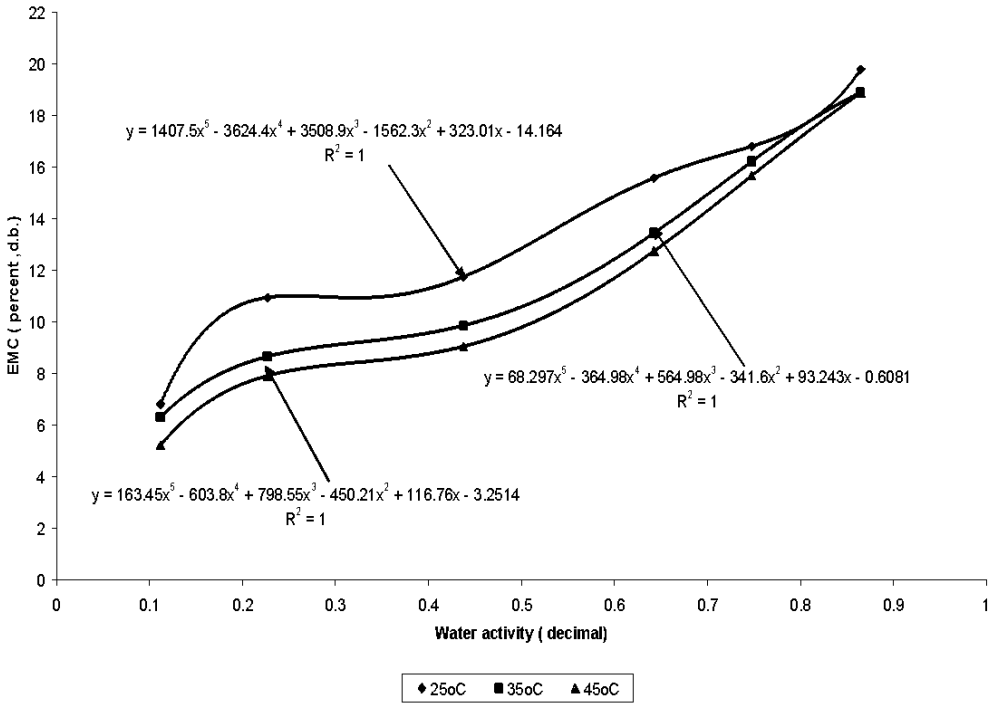

Fig 4.1 Adsorption isotherms of Tabat cultivar at three temperatures (25oC,35 oCand 45oC)

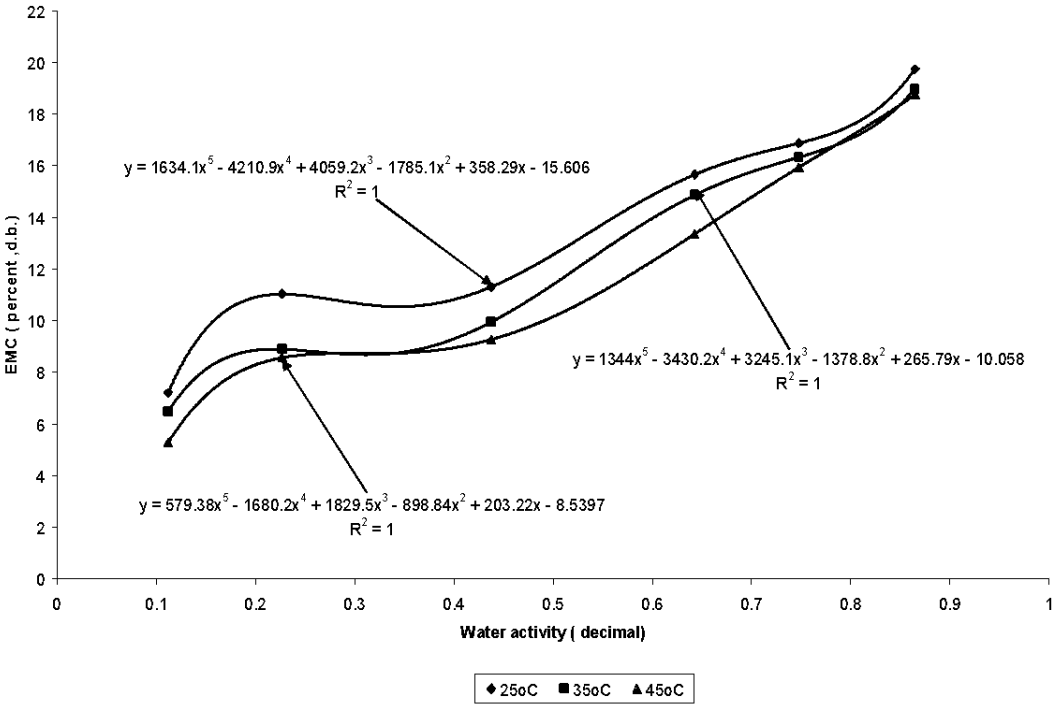

Fig 4.2 Adsorption isotherms of Wad Ahmad cultivar at temperatures (25oC,35oC and 45oC)

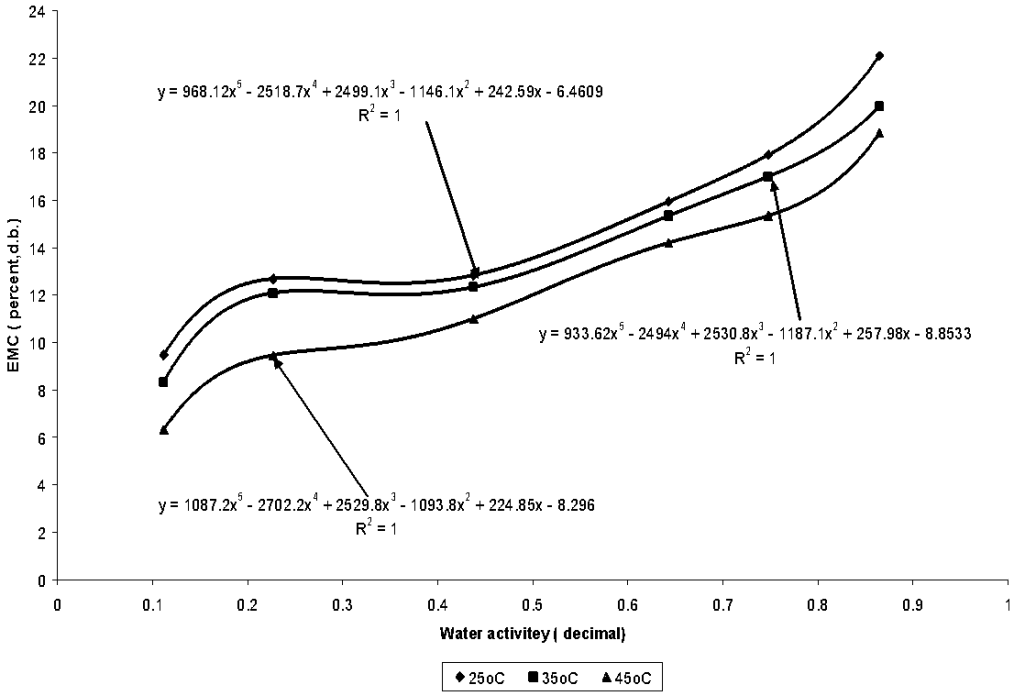

Fig 4.3 Desorption isotherms of Tabat cultivar at temperatures (25oC,35 oCand 45oC)

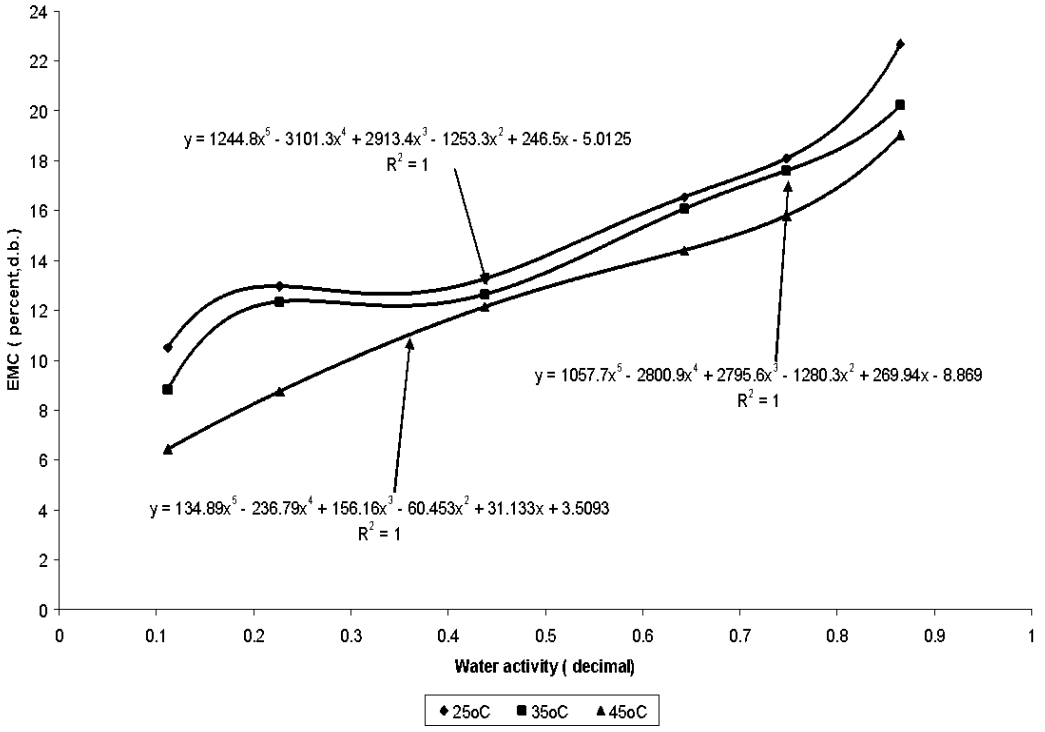

Fig 4.4 Desorption isotherms of Wad Ahmad cultivar at temperatures (25oC,35oC and 45oC)

VI. CONCLUSION

In the semi arid conditions of Sudan, the determination of moisture sorption isotherms at different temperatures and water activities to establish the correctly storage conditions for crops grains is highly needed. Wad Ahmed cultivar gave the highest values of adsorption and desorption equilibrium compared to Tabat cultivar at the same temperature and water activities. So, increasing temperature from 25°C to 45°C decreased the sorption isotherms at a constant water activity, while increasing water activities from 0.112 to 0.865 increased the sorption isotherms for both adsorption and desorption equilibrium at a constant temperature.

REFERENCES

1. Abdalla, A.T.; Stigter, C.J. and Mohammed, H.A. (2002). Traditional underground grain storage in clay soils in Sudan improved by recent innovations. Tropiculture, 20 (4): 170-175.
2. Adebo, O.A.; Njobeh, P.B.; Mulaba-Bafubiandi, A.F.; Adebiyi, J.A.; Desobgo, S.C.Z.; Kayitesi, E. (2018). Optimization of fermentation conditions for ting production using response surface methodology. *J. Food Process Preserve*. 42, 370-381.
3. AOAC (1990). Official methods of analysis. 15th eidtion Gaitherburg, DW, Washington, DC, USA, Association of Analytical Chemists.
4. Arabhosseini, A., Huisman, W., Muller, J., (2010). Modeling of the equilibrium moisture content (EMC) of Miscanthus (Miscanthus x giganteus). Biomass and Bioenergy 34, 411-416.
5. Arslan, N. and Togrul, H., (2005). Moisture sorption isotherms for crushed chillies. Biosystems Engineering, 90(1): 47–61.
6. Bianco, A.M.; Boente, G.; Pollio, M.L. and Resnik, S.L. (2007). Influence of oil content on sorption isotherms of four varieties of peanut at 25°C. *Journal of Food Engineering,* 42: 327-331.
7. Bonner I.J. and Kenney K.L. (2013). Moisture sorption characteristics and modeling of energy sorghum (Sorghum bicolor (L.) Moench). *Journal of Stored Products Research* 52 (2013) 128e136.
8. Chen, C. (2000). A rapid method to determine the sorption isotherm of peanuts. *Journal of Agricultural Engineering* Research, 75 (4): 401-408.
9. Chico-Santamarta, L., Humphries, A.C., Chaney, K., White, D.R., Magan, N., Godwin, R.J., 2011. Microbial changes during the on-farm storage of canola (oilseed rape) straw bales and pellets. Biomass and Bioenergy 35, 2939-2949.
10. Eltayeb, A.A. (1999). Some non-chemical methods of preserving sorghum grain quality during storage. M.Sc. Thesis, Faculty of Agriculture, University of Khartoum, Sudan.
11. FENNEMA, O. R. (1996). Food chemistry**.** 3rd ed. New York: Marcel Dekker, 121-122.
12. Gough, M.C. (1983). Moisture mete calibration; practical guide. Trop. Stored Prod.Inf.,46.17-24.
13. Ismail, M.A. (1994). Heat and mass transfer in wheat stored in a simulated pit. Ph.D. Thesis, Silose College, Grandfield University, U.K.
14. Kaleemullah, S. and Kaillappan, R. (2004). Moisture sorption isotherms of red chillies. Bio-system Engineering, 88 (1):95-104.
15. Mc Laughlin, C. P. and Magee, T. R. A. (1998). The determination of sorption isotherm and isosteric heats of sorption for potatoes. Journal of Food Engineering, 35:267-280.
16. Medeiros, M.L., Bartolomeu Ayrosa, A.I., Pitombo, R.N.M. and da Silva Lannes, S.C., (2006) Sorption isotherms of cocoa and cupuassu products. Journal of Food Engineering, 73: 402–406.
17. Raji, A.O and Ojediran, J.O (2011). Moisture sorption isotherms of two varieties of millet. food and bioproducts processing (8) 9: 178–184.
18. Taylor, J.R.N.; Duodu, K.G. (2017). Sorghum and millets: Grain quality characteristics and management of quality requirements. In Cereal Grains;Wrigley, C., Batey, I., Miskelly, D., Eds.; Elsevier: Amsterdam, The Nether lands; 317–351.

19. Togruel H. and Arslan, N. (2006). Moisture sorption isotherm and thermodynamic properties of walnut kernels. Journal of Stored Products Research, 43: 252-264.
20. Wolf, M.; Speiss, W.E.L.and Jung, G. (1985). Standardization of isotherm measurements. In D. Simatos and J.L. Multon (Eds.), properties of water in foods (p. 662). Dordrech: Martinus Wijhoff.

This page is intentionally left blank

Nanostructures of 2d Transition Metal Dichalcogenides for Hydrogen Generation under Alkaline Conditions: From Theoretical Models to Practical Electrocatalysts

Zhexu Xi

University of Bristol

ABSTRACT

Hydrogen has been considered as the cleanest renewable energy and the ideal alternative to fossil fuels. Electrocatalytic Hydrogen Evolution Reaction (HER) via water splitting also plays an indispensable role in high-efficiency energy con- version. Compared with the well-investigated acidic HER, the relatively slow kinetics and unclear mechanism of HER in alkaline environ- ments largely make the design of electrocatalysts a trial-and-error process, retarding the scalable development of efficient, sustainable hydrogen production. Furthermore, two-dimensional tran- sition metal dichalcogenides (2D TMDs) have been demonstrated to be promising acidic/ alkaline HER catalysts in water electrolysis due to their outstanding atom-level thickness and surface-based properties.

Keywords: alkaline HER; 2D TMDs; electrocata- lysis; surface science; structure-property correlation.

Classification: FOR Code: 291899

Language: English

London Journals Press

LJP Copyright ID: 925652
Print ISSN: 2631-8490
Online ISSN: 2631-8504

London Journal of Research in Science: Natural and Formal

Volume 21 | Issue 3 | Compilation 1.0

Nanostructures of 2d Transition Metal Dichalcogenides for Hydrogen Generation under Alkaline Conditions: From Theoretical Models to Practical Electrocatalysts

Zhexu Xi

ABSTRACT

Hydrogen has been considered as the cleanest renewable energy and an ideal alternative to fossil fuels. Electrocatalytic Hydrogen Evolution Reaction (HER) via water splitting also plays an indispensable role in high-efficiency energy conversion. Compared with the well-investigated acidic HER, the relatively slow kinetics and unclear mechanism of HER in alkaline environments largely make the design of electrocatalysts a trial-and-error process, retarding the scalable development of efficient, sustainable hydrogen production. Furthermore, two-dimensional transition metal dichalcogenides (2D TMDs) have been demonstrated to be promising acidic/alkaline HER catalysts in water electrolysis due to their outstanding atom-level thickness and surface-based properties. To minimise the gap between fundamentals and practical applications of alkali-active electrocatalysts, a class of 2D ultrathin nanomaterials show an infusive potential in identifying related key descriptors and principles. In this article, a general overview based on the principles of HER is presented, especially key parameters for evaluating the activity. Next, according to the basics of HER, the controversial mechanism of the alkaline HER process is comprehensively discussed, especially the detailed comparison with the acidic HER in three aspects: proton donors, energy barriers and roles of active sites. Then, modulation strategies of 2D TMDs for HER in electrocatalysis are analysed together with the theoretical calculations, electrochemical experiments and surface modification. Finally, an overall perspective of the rational design of highly efficient electrocatalysts under alkaline solutions in water splitting system is proposed.

Keywords: alkaline HER; 2D TMDs; electrocatalysis; surface science; structure-property correlation.

Author: Bristol Centre for Functional Nanomaterials, University of Bristol, Bristol, UK.

I. INTRODUCTION

In the 21st century, in order to reduce the reliance on less cleaning and non-renewable energy such as fossil fuels, hydrogen has been gradually widely developed as an ideal, eco- friendly source due to its high energy density and non-toxicity[1][2]. To achieve the efficient electric-to-chemical energy conversion with only water produced, water electrolysis (also known as electrochemical water splitting) is also consid- ered to be a main environmentally friendly pathway for hydrogen generation[3]. HER, one of the half-reactions in the water splitting process, occurs at anode-electrolyte interfaces. Its performance depends primarily on the catalytic reactivity of anode electrode materials as electrocatalysts[4][5]. Thus, it is of great impor- tance to explore further two questions: How do electrolyte solutions affect the HER activity and kinetics? What is the relationship between the electrocatalyst nanostructures and electroca- talytic performance?

Specifically, one of the inevitable challenges in electrocatalysis is to identify the relationship between microscopic dynamics of intermediate species or absorbed states and macroscopic

kinetics. Also, the apparent rate constant in electrocatalytic reactions usually counts on the extrinsic electrocatalyst-hydrogen interactions at electrocatalyst-electrolyte interfaces and the intrinsic electronic properties of the specific electrocatalyst. Accordingly, the electrolyte and the electrocatalyst always act together to determine the behavior of adsorbed intermediates, energy barriers and overpotential/activation energies via these extrinsic and intrinsic features[4][6]. HER is just an ideal reaction model to value the inner interdepe- ndence from a nanoscale world to real-world applications, so HER plays an momentous role in narrowing the gap between theoretical framework on surface electrolysis and practical design of electrocatalysts[7]. For instance, the combination of electrochemical measurements and surface characterisation successfully brings a wide-range relationship between surface physicochemical properties and catalytic activ- ity[8]; Similarly, in terms of the theoretical calculations, a direct quantitative model can be built between the electronic structure and appa- rent activity of an electrocatalyst[9].

The above comprehensively investigated resea- rch has largely boosted the in-depth understanding of HER in electrocatalysis, especially in acidic medium ($2H^+ + 2e^- \rightarrow H_2$), including how to identify the active sites, and how to evaluate the catalytic activity on various electrode materials for better design. Meanwhile, the alkaline HER mechanism is still under debate, mainly behind the discovery that the kinetics (regarding the higher exchange current densities j_o) in acid is 2-3 orders of magnitude faster than in alkali, thus suggesting a higher overpotential to push forward the reaction[5,10,11]. The debate mainly includes:

1) the nature of pH dependence on the HER performance[11];
2) three core descriptors: water dissociation[12], Hydrogen Binding Energy (HBE)[13], and surface H*/OH* exchange process[14].

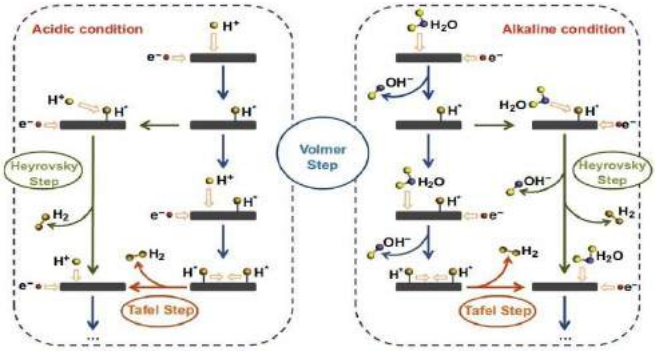

Figure 1: Schematic mechanisms of HER under acidic **(left)** and alkaline **(right)** conditions (with additional participation of dissociated water molecules as H* donors) , both containing two crucial steps: adsorption of hydrogen atoms (H*) on the active centers of electrode surface (the Volmer Step), and then generation of H_2 molecules by combination with another adsorbed H* (the Tafel Step) or with a proton from solution (the Heyrovsky Step)[15]

From **Fig. 1**, although the HER electrocatalysts act in the similar pathways in acidic and alkaline medium, the sluggish rate in alkali stems from the additional water dissociation step[15]. Consequently, to design novel, tailor-made materials for HER enhancement, these debates become emerging desires to explore how the principles of HER can be illustrated under the condition of a universal pH range (design from the science perspective), how more electrocatalytically active sites can be exposed via modified surfaces or distribution of atoms (design from the combined perspective between science and engineering), and then how morphological features can be better utilised for better apparent HER activity (design from the engineering perspective).

Recently, nanostructured metallic materials with low dimensionality has captured extensive atte-

ntion in the rational design, fabrication and characterisation of ideal HER electrocatalysts due to their high atom utilisation efficiency with strengthened electrochemical hydrogen production activity[16]. Particularly, compared with other kinds of widely applied HER electrocatalysts, 2D layered TMDs nanosheets (NSs)/nanoplates has exhibited fabulous electrocatalytic performance because of their fast electron mobility, high specific surface area, excellent surface unsaturated atoms as active sites and subsequent diversified synthesis methods[17][18]. Thus, 2D TMDs have great potential in becoming a cost-effective and highly efficient electrocatalysts for better understanding of the alkaline HER mechanisms.

Generally, it's of great value to combine theoretical calculations and experimental studies together for the rational design of 2D TMDs-based HER electrocatalysts under alkaline solutions. Here, the fundamental principles of HER process are firstly presented as well as emphasis on recent understanding and evaluation of alkaline HER. Next, the outline of 2D TMDs is highlighted to signify the structure-, surface- and morphology-related roles for connections with key activity descriptors of alkaline hydrogen generation. Then, more importantly, this systematic knowledge is extended to a broader level, which entails the design rules of practically well-defined electrocatalysts by discussing the correlations between the nanostructures of TMDs and the contributions of active sites. Finally, a personal perspective on the future feasibility in TMDs-based alkali- active electrocatalysts is proposed.

II. FUNDAMENTALS OF HER UNDER ALKALINE CONDITIONS

2.1 The role of pH in HER

Compared with the acidic and alkaline HER processes (**Fig. 1**), the sluggish rate in alkaline Medium (about 2-3 orders of magnitude lower activity than in acid medium) may originate from the additional dissociation of water to provide adsorbed H* in the Volmer reaction, thereby leading to the low concentration of H*. As water molecules become the sole proton donors in alkaline environments, the slow water dissociation step inevitably causes the slow rates in subsequent steps.

This explanation has been implicitly supported by a system of HER tests with different metallic electrodes and varying pH conditions, from acidic (pH=1-4), to neutral (pH=4-11), and to alkaline (pH=11-14) (Fig.2)[19]. Besides the demonstration of a strikingly weakened HER activity in alkali, the increasing pH up to pH=4 presents a pure diffusion limiting current different from the typical polarisation profile, accordingly revealing the characteristic change of metallic surface-specific electrode potential. This discovery signifies the key influential factors of HER process is the mass transport of H_3O^+ (hydrogen intermediate species), not the charge transfer. Also, when the electrolyte solutions become neutral or alkaline, the polarisation processes behind the current-potential curves of different electrocatalysts are clearly free from the change of pH values, indicating that currents is intimately related to pH-independent transformation from water to hydrogen molecules[19][20].

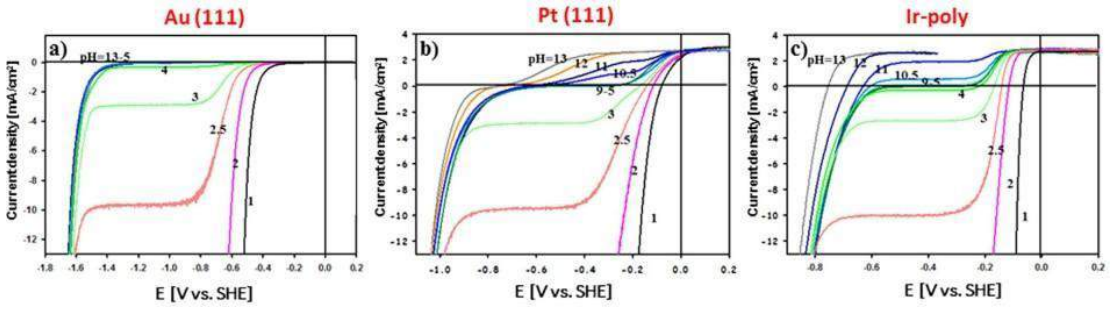

Figure 2: Polarisation (current-potential) curves for three metallic HER electrocatalysts: **a)** Au(111), **b)** Pt(111), and **c)** Ir-poly. Experimental conditions: 0.1 M $NaClO_4$ as solvents, purged with H_2, addition of NaOH or $HClO_4$ for pH adjustment. Testing conditions: rotation rates of 1600 rpm and sweep rate of 50 mV/s[19].

Overall, HER activity is seemingly pH-dependent, but the slow kinetics of alkaline HER has been demonstrated not to be entirely interpreted by the pH values near the catalyst surface. More accurate and comprehensive explanations need to be highlighted for bridging the gap between the underlying alkaline HER mechanisms and the practical design principles of electrocatalysts. Three reasonable theories are mentioned based on the current investigations: water dissociation theory, hydrogen binding energy (HBE) theory and H*/OH* or interface water transfer theory.

2.2 Water dissociation: the rate-determining step?

As mentioned in 2.1., the kinetics of alkaline hydrogen production is strictly restricted by the additional water dissociation step. Different from the high concentration of H* with H*-rich surfaces in acidic environments, water is the sole proton donor for the Volmer Reaction of alkaline/neutral HER, thus producing an extra tremendous energy barrier for cleaving H-O-H bond and generating hydrogen intermediates. As a result, water dissociation can be regarded as the rate-determining step of alkaline HER. The overall microscopic process in basic media was perfectly verified by Subbaraman et al. that $Ni(OH)_2$ clusters prompted the HER kinetics and activity by improving water dissociation for H* generation near the Pt surface[21].

Nonetheless, the water dissociation theory still cannot receive the universal acceptance in the electrocatalytic community because the experiments are conducted on the surface with high surface area, not in agreement with the ideal computational model surfaces.

2.3 Hydrogen Binding Energy: applicable under a universal range of pH?

Considering the similar HER reaction pathways in acid and alkali, the HER catalytic performance is regarded to be closely linked with HBE in all pH conditions, which can be measured on the electrode interface[13][22]. HBE is reckoned to be correlated with HER kinetics, as change of hydrogen underpotential adsorption/desorption (H_{upd}) peak positions is related to H_2 production rates. Another evidence suggests that too intense HBE results in a high energy barrier for water activation, naturally triggering sluggish kinetics of HER[22][23]. Similarly, as **Fig. 1** shows, in nanostru- ctured electrocatalysts, weaker hydrogen adsor- ption capacities bring greater exchange current densities[19][23].

However, HBE is an intrinsic parameter of catalyst, so it is pH-independent; accordingly, an assumption was proposed that HER kinetics depends on the net effect of HBE and water adsorption, and then was further demonstrated by the Goddard group that water at interfaces have different orientation with the corresponding adsorption behavior under different pH[10][24]. Specifically, more basically soluble environments bring weaker surface adsorption of water molecules and conversely promotes the strength of H-O-H bond.

Despite identification of the role of water adsorption at interfaces in pH-HBE correlation, the HBE theory cannot be the sole descriptor of HER process under all pH. The interface nanostructures of catalyst can also contribute to the HER activity. For instance, the impact of electric double layers on the HER was thoroughly studied by the Koper group that H_{upd} peak and the potential of zero charge (pzc) shift in the same way as the pH values change[25]. This indicates that the reorganisation energy can be tuned for accelerated H+/OH- migration from the surface to the bulk, thereby regulating the activation barrier for H* adsorption and HER kinetics. Specifically, alkaline medium suggests a large reorganisation energy, thereby causing a relatively slow gas production rate.

2.4 H/OH* transfer at interfaces: the competitive role of OH**

The Koper's research indicates the indispens- able role of interfacial water activation and H* adsorption for boosted HER activity. In fact, this discovery generates another viewpoint that the H*/OH* adsorption in alkaline medium are always in a race with a shared surface active site, thus decreasing the hydrogen generation rate. In addition, Liu et al. verified that cleaving OH* on catalyst surface weakens the alkaline HER kinetics on account of the absence of OH*-based interface adducts[26]. According to the two studies, although adsorption of OH* cannot participate in the Volmer Step or affect the HER activity solely, OH* mobility through the electric double layer does also play a part for HER enhancement by altering the pH-dependent density of OH^- and metal anions[19][26].

Therefore, although OH* cannot exert a direct influence on the stimulation of HER kinetics, it is still considered to have connectivity with the role of OH^- and the related sluggish alkaline HER kinetic rates. More significantly, the OH* and cations at interfaces provide a new insight into the rational design of "dual active sites" electro-catalysts. This strategy promotes the efficiency in identification of H*/OH* by creating another active site for spatial separation of the two intermediates.

2.5 Overall impact on alkaline HER

Although massive studies have been implemented to strengthen the understanding of the internal principles of alkaline HER, especially the debate on whether extra water dissociation or H* adsorption process acts decisively, there is still no answer regarding these issues on the atomic or molecular level. However, they all mentioned the additional activation barrier stemming from breaking the strong H-O-H bonds and extracting abundant intermediates from water molecules. Naturally, both theoretical and experimental studies suggest the net impact between the Gibbs Free Energy change of water dissociation and of H* (or OH*) adsorption as the key factors in alkaline HER[27]. These factors all determine the overall rate as well as the enthalpy entailing a series of energy barriers.

Hence, while in alkaline medium, the optimum reaction pathway is to minimise the energy barriers between the kinetic water dissociation and the thermodynamic H*/OH* adsorption. However, from the aforementioned debate, the effect of electrode potential and electrolyte pH can be the main factors to affect the two processes. In other words, it's extraordinarily vital to construct an efficient hydrogen evolution system considering the above factors, underlying methodologies behind the controversial theories as well as experimental data.

III. ADVANTAGES OF 2D TMDS FOR CLEARER UNDERSTANDING OF ALKALINE HER

3.1 Advantages of nanostructured 2D TMDs

2D TMDs (usually expressed in the formula of MX_2, where M=Mo, W, Ta or Nb and X=S, Se or Te), as an intriguing part in the large family of 2D nanomaterials, has drawn an increasing attention due to unique atomic and electronic structures with outstanding, surface-related preparation tec-hnologies and characterisation techniques[28].

Because of electrons strictly confined in the ultra-thin 2D space, especially for monolayered materials, the excellent structural and electronic properties of 2D TMDs could be generated.

Secondly, their great in-plane covalent bond strength and atom-level thickness contribute to appealing flexibility and mechanical strength[29]. Thirdly, their high specific area can provide plentiful active sites for boosted electrocatalysis; also, a system of mature modification strategies (e.g. stress-strain effect, heteroatom doping, defect engineering, phase transformation) help expose active facets selectively for high-selectivity catalysis. Fourthly, the surface functionalisation and the aforementioned strategies could be more easily conducted to modulate the electronic states or band structures of TMDs owing to their broad surfaces with high exposure of atoms[29][30].

3.2 How 2D TMDs contribute to structure-activity analysis

Because of high specific area and well tunable engineered structures as well as a system of various TMDs-targeted preparation technologies and characterising methods, 2D TMDs can be endowed with versatile electronic, physicochemical and surface properties, and also comprehensively understood considering several key features: sizes, shapes, compositions, thicknesses, surface states, defects, crystal phases, vacancies, strains and electronic states[6,21,29]. Similarly to the ideas of structure-activity correlations in acidic HER(Fig. 3), regulating these features can evidently optimise the activation barriers originating from the water dissociation and H* adsorption and facilitates the water dissociation step, thereby improving the HER activity in alkaline environments[2,4,31,32].

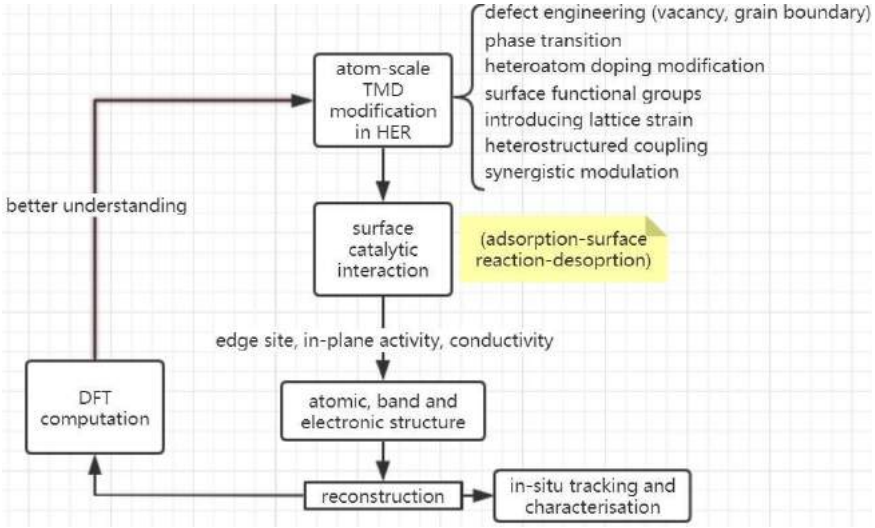

Figure 3: Schematic Principles of the Optimal Design and Modulation of TMDs-based HER Electrocatalysts in Acidic Medium[32]

To understand the structure-activity correlation more clearly, it's necessary to confirm the relationship between the surface morphology of a specific electrocatalyst and H_2 production rates. Firstly, TMDs provide a huge surface to establish the links between the kinetics and any possible parameters. Besides the aforementioned H*/OH* combination competition, water at catalyst-based interfaces, local internal electric field and solvent effect, surface H* coverage in different intensities is another factor to describe the controllable kinetics of alkaline HER by impairing the HBE since the hybridization between the s state of *H and the d band of transition metal would shift the d-band center[33]. Secondly, in various theoretical and experimental research, the role of surface defect densities and spatial distribution are highlighted as potential active sites for HER enhancement by generating a more active and well-ordered surface[5,21,28].

Consequently, the structure and morphology of TMDs provide more insights into the design of practical HER electrocatalysts. More discussions on considerations of bridging the gap between theoretical models and real-world products are required hereafter.

IV. THE RATIONAL DESIGN OF PRACTICAL TMDS-BASED ELECTROCATALYSTS IN ALKALINE HER

4.1 General guidelines of constructing an alkali-active catalysts

Although it's still unclear whether the kinetic water dissociation or the thermodynamic adsorption/desorption of activated intermediate species acts more significantly in alkaline HER, plentiful studies have established links among structural properties of TMDs, main descriptors stemming from the three controversial theories and practical efficiency in HER by analysing the involved intermediates (H_3O^+, OH^-, and other cations/anions at interfaces) with accompanying altered activation barriers[6,7,9,21-23,38]. From materials science perspectives, because H^+ and OH^- are both participators in the alkaline HER process, it's vital to optimally balance the abilities of water dissociation and H* adsorption. Accordingly, two feasible suggestions are mentioned: reducing the energy barrier thermodynamically and modulating the catalyst-hydrogen interaction kinetically. In addition, note that great physical properties of TMDs (e.g. large surface area, mechanical strength and high electron mobility) largely influence the durability and activity of catalysts[8,13,34].

Besides the thermodynamic and kinetic factors, the differentiation of theoretical and real surfaces of nanomaterials could not be ignored. Here, the most important factor is active sites. Although the broad surface endows TMDs with large numbers of active sites, coverage of adsorbed H*/OH* could decrease the densities of available sites on the surface[19][35].

Moreover, not all defect states might be active centers for HER optimisation, so the tailored surface morphology with well-defined arrangement of defects could have a different impact on HER compared with the ideal surface[23][36].

4.2 The proton donor and generation of energ barrier from activation

All of the three theories have emphasised a tailor-made reaction pathway to connect the change of activation barriers with two thermodynamic states entailing water molecules, H*, OH* and other potential cations/anions at catalyst-electrolyte interfaces. This is closely related to the dissociated water for donating protons and the adsorbed hydrogen intermediates for formation of the activated hydrogen-catalyst complexes[21][33].

No matter the origin of H* is H_2O or H_3O^+, the H* discharge process in alkaline media is too slow to be tracked experimentally by the water dissociation mechanism[37]. The drastic change presented in the polarisation curve is the total effect of H*, OH*, and other existing proton donors in electrolytes like HSO_4^- and HCO_3^-[38]. Thus, the additional water dissociation step could tune the subsequent intermediate formation and even be the rate-determining step to facilitate the entire kinetics.

As for thermodynamic adsorption/desorption processes, to promote the subsequent reactions, the bond of H* and OH* bound to the catalyst surface is required not to be too strong or too weak. The TMD-based electrocatalysts should possess bi-functionality to keep a balanced binding strength at interfaces as well as the proper degree of surface coverage between two kinds of intermediate species[19]. Accordingly, proper partition of surface bonding with H* and OH* spectators could tune the activation barrier, thereby optimising the adsorption/desorption process and achieving the enhanced HER efficiency.

4.3 Well-defined TMDs nanosurface with well-organised active sites: connections between ideal models and practical catalysts

4.3.1 Different surface of ideal and realistic TMDs-based electrocatalysts

The aforementioned various kinds of species and the hydrogen/hydroxyl-catalyst interactions are highly sensitive to the local atom-thin structure of TMDs, triggering the structurally sensitive HER process[23][36]. In addition, nanostructures with high surface area are urgently required to enhance the specific activity for the practical use of energy conversion devices. Note that the realistic existence of edges and defects can be potential catalytically active centers to modulate the electronic structures or band levels of TMDs-based electrocatalysts. More importantly, the spatial orientation and distribution of surface defects can tune the alkaline HER activity by regulating the interface interaction of H*/OH* spectators[30][37].

Therefore, both the theoretical insights of surface-sensitive dynamics should be extended to a more real-life level in agreement with the experimental results of TMDs-related electrocatalysis. This link could be ascribed to a well-defined nanoscale and ordered nanostructure with great crystallinity derived from the systematic calculation considering morphological features on the catalyst surface like facets, edges, step sites and corners.

4.3.2 Core idea: optimising the availability of available active sites

For the purpose of strengthening the electrocatalytic HER performance as well as achieving the expected consistency between the macroscopic HER activity and the microscopic 2D structural factors, diversified nanosurfaces are constructed via versatile modification methods such as heteroatom doping, defect/disorder engineering and vertically arrayed heterostructure construction[38]. With these methods, the surface adsorption energetics is changed by altering the electronic structures and simultaneously, more available active sites could be exposed or created, forming a type of synergistic coordination. Further, a more in-depth insight has been proposed and afterwards demonstrated that the entire alkaline HER activity is determined by a combined effect of H* adsorption and OH* desorption[39]. This opinion indicates a balance between the transition state energy of water molecules and the final state energy of H*/OH* "spectator" species, and highlights the bi-functionality of active sites, also suggesting the validity of these modification methods in 2D TMDs-related structure-activity analysis.

Moreover, by monitoring the surface-controlled or structural parameters, the coordination environment (containing orientation, local density and distribution) and function (dependent on the categories of reaction intermediates) of active sites on the TMDs surfaces/interfaces can be precisely tuned. Theoretically, entirely different from H* as the sole intermediate in acid, there might be a surfeit of various species in alkaline medium: H*, OH*, H_2O, other electrolyte-related anions/cations[6,8,10,12,19-21,37]. In other words, diversified spectators can form the bond with different kinds and strengths at interfaces, so more complicated species and energy change will be taken into account in the design and engineering of active sites.

4.3.3 The roles of available active sites in design and engineering

Under the principles of the experimental and theoretical considerations mentioned above, the availability of active roles plays a crucial role in the rational design of TMDs-based electrocatalysts, especially in terms of the homogeneity of electrocatalysts with tailored surfaces or nanostructures[19,37].

Firstly, the systematic design must be built on the studies of extended interfaces. Usually, based on the introduction of active sites, the correlation between coordination environment, binding energies and practical activity can be observed to better predict an ideal geometric environment of the sites[40]. Specifically, the measured coordination number of the surface sites can be closer to the optimum value by mobilising the second nearest atoms for modified coordination of nearest atoms.

Other similar strategies based on the formation of ordered surfaces with reduced bulk surfaces can contribute to the maximum exposure of well-organised sites as well as optimised geometric environments and altered electronic states. Further, the construction of various active sites may result in more disordered surfaces such as typically more active edge sites and relatively inert in-plane sites of TMDs, representing an extraordinarily high initial activity and stability[41,42]. The disordered surfaces can provide an efficient route for the design of alkali-active and durable electrocatalysts.

Thus, the rational design of TMDs-based electrocatalysts requires mild binding energy and a proper coordination environment, especially entailing the particle interactions at the electrolyte-catalyst interfaces, for better activity, durability and selectivity.

V. SUMMARY AND PERSPECTIVES

The origin of pH-dependent hydrogen evolution kinetics is the synergistic result of H* surface coverage, water molecules at interfaces and H*/OH*-catalyst bonds. The sluggish rate of HER in alkaline medium is due to the additional water dissociation step and the subsequent adsorption energetics. By providing a detailed explanation of three controversial theories and analysing the structure-activity correlations in terms of the critical descriptors stemming from the theories (source of donated protons, formation of activation barriers and active sites from the interactions at interfaces), the combinations of theoretical and experimental studies are summarised to bridge the gap between the calculated models and the real-life applications of electrocatalysts. Following the structure-descriptor-activity guidelines, TMDs with 2D well-defined nanostructures, atom-level thickness and a high specific surface area have been demonstrated to be alkali-active and stable electrocatalysts, in agreement with the theoretical induction and experimental results.

However, because of the complicated models entailing various intermediates and unpredictable energy change between thermodynamic states, a more accurate in-situ tracking and characterisation system can be developed to confirm the real-time interactions between electrocatalysts and intermediates. Note that the local environment at interfaces and the mass transport kinetics need to be highlighted as two extra important factors. Also, to make the theoretical calculations closer to experimental results, more precisely tunable crystal surfaces with nanostructures should be taken into account in terms of size, shape, defects, phase structure and crystallinity.

Finally, the role of electric double layers is mentioned, but till now, no targeted research in revealing its function in optimising the mobility of ions across the layers has been conducted. The relationship between surface properties of electrocatalysts and the layers needs a more comprehensive understanding.

REFERENCES

1. Wu, M.; Zhang, J.; He, B. -B.; Wang, H. -W.; Wang, R.; Gong, Y.-S. In-Situ Construction of Coral-Like Porous P-Doped g-C_3N_4 Tubes with Hybrid 1D/2D Architecture and High Efficient Photocatalytic Hydrogen Evolution. Appl. Catal. B: Environ. **2019,** 241, 159-166.
2. Zheng, Y.; Jiao, Y.; Jaroniec, M.; Qiao, S. Advancing the Electrochemistry of the Hydrogen-Evolution Reaction through Combining Experiment and Theory. Angew. Chem. Int. Ed. **2015**, 54, 52-65.
3. Zhang, J.; Wang, T.; Liu, P.; Liu, S.; Dong, R.; Zhuang, X.; Chen, M.; Feng X. Engineering Water Dissociation Sites in MoS_2 Nanosheets for Accelerated Electrocatalytic Hydrogen Production. Energy Environ. Sci. **2016**, 9, 2789-2793.
4. Zhou, M.; Weng, Q.; Zhang, X.; Wang, X.; Xue, Y.; Zeng, X.; Bando, Y.; Golberg, D. In Situ Electrochemical Formation of Core-Shell Nickel-Iron Disulfide and Oxyhydroxide Heterostructured Catalysts for a Stable Oxygen Evolution Reaction and the Associated Mechanisms. J. Mater. Chem. A **2017**, 5, 4335-4342.
5. Miao, M.; Pan, J.; He, T.; Yan, Y.; Xia, B.; Wang, X. Molybdenum Carbide-Based Elec-

trocatalysts for Hydrogen Evolution Reaction. Chem. Eur. J. **2017**, 23, 10947-10961.
6. Strmcnik, D.; Lopes, P.; Genorio, B.; Stamenkovic, V.; Markovic, N. Design Principles for Hydrogen Evolution Reaction Catalyst Materials. Nano Energy **2016**, 29, 29-36.
7. Jiao, Y.; Zheng, Y.; Jaroniecb, M.; Qiao, S. Design of Electrocatalysts for Oxygen and Hydrogen-Involving Energy Conversion Reactions. Chem. Soc. Rev. **2015**, 44, 2060-2086.
8. Stamenkovic, V.; Strmcnik, D.; Lopes, P.; Markovic, N. Energy and Fuels from Electrochemical Interfaces. Nature Mater. **2017**, 16, 57-69.
9. Skúlason, E.; Jónsson, H. Atomic Scale Simulations of Heterogeneous Electrocatalysis: Recent Advances. Adv. Phys. **2017**, 2, 481-495.
10. Schmidt, T.; Ross Jr., P.; Markovic, N. Temperature Dependent Surface Electrochemistry on Pt Single Crystals in Alkaline Electrolytes: Part 2. The Hydrogen Evolution / Oxidation Reaction. J. Electroanal. Chem. **2002**, 524-525, 252-260.
11. Jia, Q.; Liu, E.; Jiao, L.; Li, J.; Mukerjee, S. Current Understandings of the Sluggish Kinetics of the Hydrogen Evolution and Oxidation Reactions in Base. Curr. Opin. Electrochem. **2018**, 12, 209-217.
12. Subbaraman, R.; Tripkovic, D.; Strmcnik, D.; Chang, K. -C.; Uchimura, M.; Paulikas, A.; Stamenkovic, V.; Markovic, N. Enhancing Hydrogen Evolution Activity in Water Splitting by Tailoring Li^{+}-$Ni(OH)_2$-Pt Interfaces. Science **2011**, 334, 1256-1260.
13. Durst, J.; Siebel, A.; Simon, C.; Hasché, F.; Herranz, J.; Gasteiger, H. A. New Insights into the Electrochemical Hydrogen Oxidation and Evolution Reaction Mechanism. Energy Environ. Sci. **2014**, 7, 2255-2260.
14. Janik, M.; McCrum, I.; Koper, M. On the Presence of Surface Bound Hydroxyl Species on Polycrystalline Pt Electrodes in the "Hydrogen Potential Region" (0–0.4 V-RHE). J. Catal. **2018**, 367, 332-337.
15. Wei, J.; Zhou, M.; Long, A.; Xue, Y.; Liao, H.; Wei. C.; Xu, Z. Heterostructured Electrocatalysts for Hydrogen Evolution Reaction Under Alkaline Conditions. Nano-Micro Lett. **2018**, 10, 75.
16. Zhao, X.; Dai, L.; Qin, Q.; Pei, F.; Hu, C.; Zheng, N. Self-Supported 3D PdCu Alloy Nanosheets as a Bifunctional Catalyst for Electrochemical Reforming of Ethanol. Small **2017**, 13, 1602970.
17. Ding, Q.; Song, B.; Xu, P.; Jin, S. Efficient Electrocatalytic and Photoelectrochemical Hydrogen Generation Using MoS_2 and Related Compounds. Chem **2016**, 1, 699-726.
18. Garlyyev, B.; Fichtner, J.; Piqué, O.; Schneider, O.; Bandarenka, A. S.; Calle-Vallejo, F. Revealing the Nature of Active Sites in Electrocatalysis. Chem. Sci. **2019**, 10, 8060-8075.
19. Strmcnik, D.; Uchimura, M.; Wang, C.; Subbaraman, R.; Danilovic, N.; van der Vliet, D.; Paulikas, A.; Stamenkovic, V.; Markovic, N. Improving the Hydrogen Oxidation Reaction Rate by Promotion of Hydroxyl Adsorption. Nat. Chem. **2013**, 5, 300-306.
20. Zeng, Z.; Chang, K.; Kubal, J.; Markovic, N.; Greeley, J. Stabilization of Ultrathin (Hydroxy) Oxide Films on Transition Metal Substrates for Electrochemical Energy Conversion. Nat. Energy **2017**, 2, 17070.
21. Subbaraman, R.; Tripkovic, D.; Strmcnik, D.; Chang, K. -C.; Uchimura, M.; Paulikas, A.; Stamenkovic, V.; Markovic, N. Enhancing Hydrogen Evolution Activity in Water Splitting by Tailoring Li+-Ni (OH)2-Pt Interfaces. Science **2011**, 334, 1256-1260.
22. Sheng, W.; Zhuang, Z.; Gao, M.; Zheng, J.; Chen, J.; Yan, Y. Correlating Hydrogen Oxidation and Evolution Activity on Platinum at Different pH with Measured Hydrogen Binding Energy. Nat. Commun. **2015**, 6, 5848.
23. Zheng, J.; Sheng, W.; Zhuang, Z.; Xu, B.; Yan, Y. Universal Dependence of Hydrogen Oxidation and Evolution Reaction Activity of Platinum-Group Metals on pH and Hydrogen Binding Energy. Sci. Adv. **2016**, 2, No. e1501602.
24. Cheng, T.; Wang, L.; Merinov, B.; Goddard, W. Explanation of Dramatic pH-Dependence of Hydrogen Binding on Noble Metal Electrode: Greatly Weakened Water Adsorption at High pH. J. Am. Chem. Soc. **2018**, 140, 7787-7790.

25. Ledezma-Yanez, I.; Wallace, W.; Sebastián Pascual, P.; Climent, V.; Feliu, J.; Koper, M. Interfacial Water Reorganization as a pH-Dependent Descriptor of the Hydrogen Evolution Rate on Platinum Electrodes. Nature Energy **2017**, 2, 1-7.
26. Liu, E.; Li, J.; Jiao, L.; Doan, H.; Liu, Z.; Zhao, Z.; Huang, Y.; Abraham, K.; Mukerjee, S.; Jia, Q. Unifying the Hydrogen Evolution and Oxidation Reactions Kinetics in Base by Identifying the Catalytic Roles of Hydroxyl-Water-Cation Adducts. J. Am. Chem. Soc. **2019**, 141, 3232-3239.
27. Skúlason, E.; Tripkovic, V.; Bjo¨rketun, M.; Gudmundsdottir, S.; Karlberg, G.; Rossmeisl, J.; Bligaard, T.; Jónsson, H.; Nørskov, J. Modeling the Electrochemical Hydrogen Oxidation and Evolution Reactions on the Basis of Density Functional Theory Calculations. J. Phys. Chem. C **2010**, 114, 18182-18197.
28. Tan, C.; Cao, X.; Wu, X. -J.; He, Q.; Yang, J.; Zhang, X.; Chen, J.; Zhao, W.; Han, S.; Nam, G. -H.; Sindoro, M.; Zhang, H. Recent Advances in Ultrathin Two-Dimensional Nanomaterials. Chem. Rev. **2017**, 117, 6225-6331.
29. Guo, Y.; Xu, K.; Wu, C.; Zhao, J.; Xie, Y. Surface Chemical Modification for Engineering the Intrinsic Physical Properties of Inorganic Two-Dimensional Nanomaterials. Chem. Soc. Rev. **2015**, 44, 637-646.
30. Fu, Q.; Han, J.; Wang, X.; Xu, P.; Yao, T.; Zhong, J.; Zhong, W.; Liu, S.; Gao, T.; Zhang, Z.;Xu, L.; Song, B. 2D Transition Metal Dichalcogenides: Design, Modulation, Challenges in Electrocatalysis. Adv. Mater. **2021**, 33, 1907818.
31. Liu, Y.; Wu, J.; Hackenberg, K.; Zhang, J.; Wang, Y.; Yang, Y.; Keyshar, K.; Gu, J.; Ogitsu, T.; Vajtai, R. Self-Optimizing, Highly Surface-Active Layered Metal Dichalcogenide Catalysts for Hydrogen Evolution. Nat. Energy **2017**, 2, 17127.
32. Xi, Z. Underlying Structure-Activity Correlations of 2D Layered Transition Metal Dichalcogenides-Based Electrocatalysts for Boosted Hydrogen Generation. arXiv preprint **2021**, arXiv: 2103. 02441.
33. Zhu, S.; Qin, X.; Yao, Y.; Shao, M. pH-Dependent Hydrogen and Water Binding Energies on Platinum Surfaces as Directly Probed Through Surface-Enhanced Infrared Absorption Spectroscopy. J. Am. Chem. Soc. **2020**, 142, 8748-8754.
34. Jiao, Y.; Zheng, Y.; Jaroniec, M.; Qiao, S. Design of Electrocatalysts for Oxygen- and Hydrogen-Involving Energy Conversion Reactions. Chem. Soc. Rev. **2015**, 44, 2060-2086.
35. Eng, A. Y. S.; Ambrosi, A.; Sofer, Z.; Simek, P.; Pumera, M. Electrochemistry of Transition Metal Dichalcogenides: Strong Dependence on the Metal-To-Chalcogen Composition and Exfoliation Method. ACS Nano **2014**, 8, 12185-12198.
36. Zhuang, P.; Sun, Y.; Dong, P.; Smith, W.; Sun, Z.; Ge, Y.; Ye, M. Revisiting the Role of Active Sites for Hydrogen Evolution Reaction Through Precise Defect Adjusting. Adv. Funct. Mater. **2019**, 29, 1901290.
37. Li, D.; Wang, C.; Strmcnik, D.; Tripkovic, D.; Sun, X.; Kang, Y.; Chi, M.; Snyder, J.; van der Vliet, D.; Tsai, Y.; Stamenkovic, V.; Sun, S.; Markovic, N. Functional Links Between Pt Single Crystal Morphology and Nanoparticles with Different Size and Shape: The Oxygen Reduction Reaction Case. Energy Environ. Sci. 2014, 7, 4061-4069.
38. Deng, J.; Li, H.; Xiao, J.; Tu, Y.; Deng, D.; Yang, H.; Bao, X. Triggering the Electrocatalytic Hydrogen Evolution Activity of the Inert Two-Dimensional MoS_2 Surface Via Single-Atom Metal Doping. Energy Environ. Sci. **2015**, 8, 1594-1601.
39. Subbaraman, R.; Tripkovic, D.; Chang, K.; Strmcnik, D.; Paulikas, A.; Hirunsit, P.; Chan, M.; Greeley, J.; Stamenkovic, V.; Markovic, N. Trends in Activity for the Water Electrolyser Reactions on 3d M(Ni,Co,Fe,Mn) Hydr(oxy) oxide Catalysts. Nat. Mater. **2012**, 11, 550-557.
40. Wang, H.; Ming, M.; Hu, M.; Xu, C.; Wang, Y.; Zhang, Y.; Gao, D.; Bi, J.; Fan, G.; Hu, J. Size and Electronic Modulation of Iridium Nanoparticles on Nitrogen-Functionalized Carbon Toward Advanced Electrocatalysts for Alkaline Water Splitting. ACS Appl. Mater. Interfaces **2018**, 10, 22340-22347.

41. Garlyyev, B.; Kratzl, K.; Rück, M.; Michalička, J.; Fichtner, J.; Macak, J.; Kratky, T.; Günther, S.; Cokoja, M.; Bandarenka, A.; Gagliardi, A.; Fischer, R. Optimizing the Size of Platinum Nanoparticles for Enhanced Mass Activity in the Electrochemical Oxygen Reduction Reaction. Angew. Chem. Int. Ed. **2019**, 58, 9596-9600.
42. Garlyyev, B.; Fichtner, J.; Piqué, O.; Schneider, O.; Bandarenka, A.; Calle-Vallejo, F. Revealing the Nature of Active Sites in Electrocatalysis. Chem. Sci. **2019**, 10, 8060-8075.

Inhibition effects of aqueous extracts of coir pith and composted coir pith on germination and seedling growth of Rice (*oryza Sativa*), Black gram (*vigna Mungo*), and Green gram (*vigna radiata*)

Anbarasu Mariyappillai, Gurusamy Arumugam, Swaminathan Chitraputhira Pillai, Durai Singh Ramiah

Agricultural University

ABSTRACT

Aim: To evaluate the inhibition effects of aqueous extracts of coir pith and composting coir pith on Rice (Oryza sativa), Black gram (Vigna mungo), and Green gram (Vigna radiata) by response index method.

Methodology: The coir pith and composted coir pith soaked the ratio of 1:10 for 24 hrs, filtered through Whatman No.1 filter paper. The inhibition effect tested for germination and seedling growth of Rice, Black gram, and Green gram was sown in poly pots. The Carbon: Nitrogen ratio and the total organic carbon analyzed by Dry combustion method, Kjeldahl method, and GCMS/MS analysis.

Keywords: Inhibition effect, Coir pith, Composted coir pith, Response index, C: N ratio.

Classification: FOR Code: 291899p

Language: English

London Journals Press

LJP Copyright ID: 925652
Print ISSN: 2631-8490
Online ISSN: 2631-8504

London Journal of Research in Science: Natural and Formal

Volume 21 | Issue 3 | Compilation 1.0

Inhibition effects of aqueous extracts of coir pith and composted coir pith on germination and seedling growth of Rice (*oryza Sativa*), Black gram (*vigna Mungo*), and Green gram (*vigna radiata*)

Anbarasu Mariyappillai[α], Gurusamy Arumugam[σ], Swaminathan Chitraputhira Pillai[ρ] & Durai Singh Ramiah[Ꞷ]

ABSTRACT

Aim: To evaluate the inhibition effects of aqueous extracts of coir pith and composting coir pith on Rice (Oryza sativa), Black gram (Vigna mungo), and Green gram (Vigna radiata) by response index method.

Methodology: The coir pith and composted coir pith soaked the ratio of 1:10 for 24 hrs, filtered through Whatman No.1 filter paper. The inhibition effect tested for germination and seedling growth of Rice, Black gram, and Green gram was sown in poly pots. The Carbon: Nitrogen ratio and the total organic carbon analyzed by Dry combustion method, Kjeldahl method, and GCMS/MS analysis.

Results: The phytotoxic substances are present in coir pith, which can be exterminated by composting the coir pith for better growth and development of seedlings.

Interpretation: The negative response index (RI), high C: N ratio and chemical compounds like Tocopherol, Fucoxanthin, Tetramethyl Heptadecane, Dichloroacetamide, Tetrazole, Hydroxyethyl palmitate, Neocurdione, and Uridine derivations present in raw coir may have the phytotoxic effect of yellowing symptoms in young plants compared to composted coir pith. This is exterminated by composting the coir pith for better growth and development of seedlings as well as used for various agricultural and horticultural nurseries.

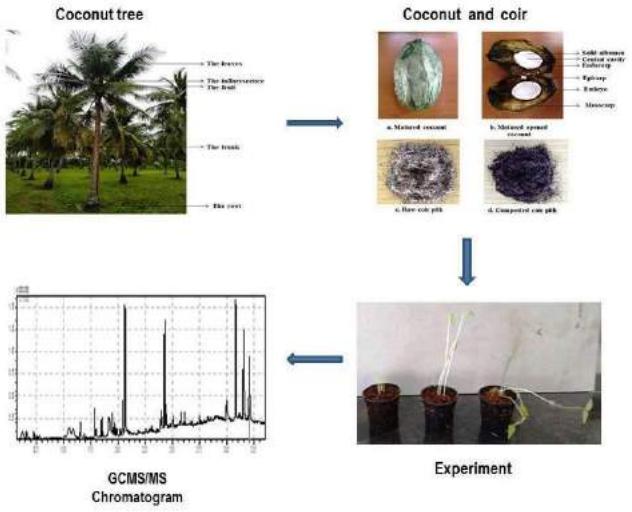

Graphical abstract

Keywords: Inhibition effect, Coir pith, Composted coir pith, Response index, C: N ratio.

Author α: Post Doctoral Fellow, Department of Agronomy, Agricultural College and Research Institute, Tamil Nadu Agricultural University, Madurai - 625 104, Tamil Nadu, India

σ: Professor and Head, Dry land Agricultural Research Station, Tamil Nadu Agricultural University, Chettinad - 630 102, Sivagangai, Tamil Nadu, India

ρ: Professor of Agronomy, Department of Agronomy, Agricultural College and Research Institute, Tamil Nadu Agricultural Unive- rsity, Madurai - 625 104, Tamil Nadu, India.

Ꞷ: Professor and Head, Department of Agronomy, Agricultural College and Research Institute, Tamil Nadu Agricultural Unive- rsity, Madurai - 625 104, Tamil Nadu, India.

London Journal of Research in Science: Natural and Formal

I. INTRODUCTION

Coir is a 100% natural happening fiber got from an inexhaustible asset of coconut husk. Coir strands take after the wood filaments regarding actual properties and compound organization. Coconut strands are seen firmly stuffed alongside non-sinewy, cushioned, and lightweight corky material known as coir substance or coir dust, which comprises around 50-70 percent of the husk. The elastic material that ties the coir fiber in the husk is the coir pith. Coir pith is currently utilized as a medium for seedling nurseries, for bedding plants, for preparing blend supplies for arranging, and for aqua-farming creation of blossoms, vegetables, trees, bushes, manure receptacles, compartment cultivating, packaging layer for mushroom. As of now, coir pith stands apart as the eco-accommodating and more dependable swap for the sphagnum peat greenery, rock fleece, and sawdust. Coir pith based items give a superb developing and pulling mechanism for hydroponics or container-based plant development. Wide variations in the C: N ratio of coir pith from 58:1 to 112:1 has been accounted for. Coir pith obtained from fully mature nuts has higher amounts of lignin and cellulose and a lesser amount of water-soluble salts compared to younger nuts. The coir pith is used as a medium of mat nursery for the germination of paddy seeds and seedling production. Mat nursery seedlings are used for machine transplanting of rice cultivation. Using coir pith affected seed germination and seedling growth and had the least values for germination, growth, and physiological parameters in rice by mat nursery. The application of raw coir pith in nursery preparation of rice and pulses to inhibit plant growth due to the wide C: N ratio, polyphenols, and phenolic acids can be made plants develop toxic yellowing phytotoxic symptoms.

II. MATERIALS AND METHODS

The inhibition effects of aqueous extract of coir pith have experimented at the Department of Agronomy, Agricultural College and Research Institute, Tamil Nadu Agricultural University, Madurai, Tamil Nadu, India located at 9˚54'N latitude and 78˚54'E longitude.

The coir pith and composted coir pith soaked separately in distilled water at a weight/volume ratio of 1:10 for 24 hrs. This ratio produces low osmolality. After 24 hours, the aqueous extracts were filtered through Whatman No.1 filter paper. The aqueous extracts were filtered and tested for inhibition of germination and seedling growth of Rice (*Oryza sativa* L.), Black gram (*Vigna mungo* (L.) Hepper), and Green gram (*Vigna radiata* (L.) R. Wilczek). Twenty-five seeds were sown in poly pots of 25 × 25 cm size, filled with coir pith. The poly pots were added with the aqueous extracts frequently to avoid drying up. Distilled water served as control. The germination (%), shoot length (cm), root length (cm), fresh weight (mg), and dry weight (mg) in rice, black gram, and green gram were recorded after two weeks. The magnitude of inhibition versus simulation in the bioassay was compared through the Response Index (RI) (Richardson and Williamson, 1988) is determined as follows,

$$\text{if } T > C,\ RI = 1 - (C/T)$$
$$\text{if } T = C,\ \text{then } RI = 0$$
$$\text{if } T < C,\ \text{then } RI = (T/C) - 1$$

Where T is the treatment mean and C is the control mean. A negative RI reflects the proportional disparity in output (germination (%), shoot length (cm), root length (cm), fresh weight (mg), and dry weight (mg)) of test crop in the treatment relative to output in the control. the results were subjected to an analysis of variance (Ayeni *et al.*, 1997), and mean RI values were tested for standard error.

The total organic carbon content in coir pith was analyzed through Dry combustion method at 540◦C for 4 hr [19] and total nitrogen content by the Kjeldahl method (Bremmer and Mulvaney, 1982).

For analyzing the chemical compounds present in the coir pith, GCMS/MS analysis was done. A volume of 1 micro lit of clear extract was injected into GCMS/MS with an oven programming of 80°C @ 5°C/min to 250°C (10 min). The injector temperature was maintained at 220°C with the detector temperature of 250 °C. The carrier gas used in the analysis was helium which had a flow

rate of 1ml/min. A 30 m length of capillary column HP5 Polar type was used. The GCMS/MS analysis was done at the Department of Agricultural Entomology, Agricultural College and Research Institute, Tamil Nadu Agricultural University, Madurai.

For identification of the components, interpretation on mass spectrum GCMS/MS was conducted using the database of national institute standard and technology (NIST) having more than 62,000 patterns. The spectrum of the unknown component was compared with the spectrum of the known components stored in the NIST library. The name, molecular weight, and structure of the component of the test materials were ascertained.

The Coir pith was composted by inoculating with a proprietary bio-formulation, such as PITH PLUS (*Pleurotus sajor caju*), and enriched with urea show a definite reduction in lignin and cellulose contents with an increase in total nitrogen and other nutrient elements after 30 days.

III. STATISTICAL ANALYSIS

The results for each characterization data were obtained from the mean procedure of three replicates and statistical analysis was performed in a complete randomization design. The data on various parameters studied during the investigation were statistically analyzed by applying the technique of standard error deviation (±), as suggested by Gomez and Gomez, (1984).

IV. RESULTS AND DISCUSSION

Carbon to Nitrogen ratio (C: N) is a ratio of the mass of carbon to a mass of nitrogen in a substance. For example, a C: N of 10:1 means there are ten units of carbon for each unit of nitrogen in the substance. Since the C: N ratio is the key factor that decides the decomposition of the organic material which can have a significant effect on the rate of decomposition, crop nutrient cycling (predominantly nitrogen), and soil nutrient availability. In the raw coir pith C: N ratio of more than 40:1 cause's nutrition disorder thus becoming yellowing of young plants. This is also invigorated by coir pith dust chemical composition. In forestry products (bark, sawdust, and woodchips) as well as compost container substrates can invite problems of phytotoxicity, which is largely depending on the chemical composition of the substrate, which in turn can cause salinity, nutritional disorders, and enzymatic or hormonal metabolic alterations (Ortega et al., 1996). High potassium and manganese content (Maher and Thomson, 1991) and the presence of phenolic compounds are terpenes, organic acids, and fatty acids (Morel and Guillemain, 2004) can also be the cause of such problems (Gruda *et al.,* 2009).

Whereas in coir pith composted using PITH PLUS (*Pleurotus sajor caju*), the C: N ratio 19:1 were balanced and nutrients are available to the plants (Table 1) as it was inoculated with bio-formulations involving e addition of supplemental substances to substrates to eliminate the "weaknesses" of natural wooden materials like coir pith, hydrolysis of woodchips under pressure in the presence of acids (Lemaire *et al.,* 1989). Using this method, the lignin-cellulose ratio was changed from 1: 2-3 to 1: 1-2. The supply of nitrogen and other mineral additives before manufacturing fiber substrates under high pressure and heat in the presence of water vapor, to improve substrate properties, is called "impregnation (Penningsfeld, 1992).

The germination and seedling growth of rice, black gram, and green gram were inhibited by coir pith and composted coir pith aqueous extracts compared to the distilled water. Raw coir pith aqueous extracts had a more inhibitory effect on rice, black gram, and green gram when compared to the composted coir pith aqueous extracts. The inhibition is due to phytotoxins present in the extracts, instead of osmotic inhibition because the use of 10 % extract ensures low osmolality (Orwa *et al.,* 2009). The readily visible effects include inhibited or retarded germination rate (Williamson et al., 1992), seeds darkening and swelling, reduced root or radicle and shoot or coleoptile extension (Turk and Tawaha, 2003; Bhatt and Todaria, 1990), swelling or necrosis of root tips, curling of the root axis, discoloration, lack of root hairs, reduced dry weight accumulation and lowered reproductive capacity (Ayeni *et al.,* 1997).

Table 1: The C: N ratio of coir pith and compost coir pith

Parameters	Coir pith	Compost coir pith
TOC (%)	59.39	30.80
Total N (100 g)	0.84	0.94
C:N ratio	40:1	19:1

The inhibition measured by RI means ranged from percentage (Figure 1). The coir pith aqueous extracts had highest suppression of germination (65.00, 46.00 and 51.00 %), root length (10.31, 5.06 and 7.55 cm), shoot length (9.21, 11.07 and 13.60 cm) Fresh weight (0.073, 0.169 and 0.332 mg) and Dry weight (0.012, 0.010and 0.018 mg) of rice, black gram and green gram respectively. It was compared to aqueous extracts composted coir pith and distilled water. (Table 2).

Table 2. Inhibition effect of rice, black gram, and green gram germination and seedling growth

	Coir pith				
	Germination %	Root length (cm)	Shoot length (cm)	Fresh weight (mg)	Dry weight (mg)
Rice	65.00±0.428	10.31±1.175	9.21±1.909	0.073±0.006	0.012±0.001
Black gram	46.00±0.173	5.06±1.703	11.07±3.707	0.169±0.058	0.010±0.003
Green gram	51.00±0.690	7.55±1.090	13.60±2.716	0.332±0.042	0.018±0.004
Composted coir pith					
Rice	69.00±0.823	12.76±1.470	11.76±1.670	0.089±0.010	0.013±0.001
Black gram	51.42±0.884	5.47±1.519	11.59±3.938	0.247±0.061	0.015±0.005
Green gram	60.00±0.730	7.91±0.936	17.99±2.294	0.392±0.053	0.016±0.005
Distilled water					
Rice	84.00±0.163	10.430±1.357	8.55±0.915	0.079±0.006	0.013±0.001
Black gram	80.00±0.149	7.470±1.306	18.56±2.843	0.307±0.058	0.014±0.003
Green gram	70.00±0.843	9.970±1.455	15.30±3.133	0.263±0.064	0.014±0.004

Data are the mean values of three replicates with±standard error

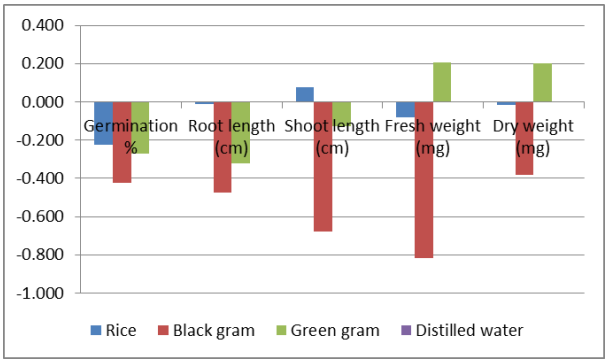

Figure 1: Response index values of coir pith on rice, black gram, and green

The RI indicated the highest negative (-) values coir pith aqueous extracts of germination (-0.226, -0.425, and -0.271), root length (-0.012, -0.476, and -0.321) of rice, black gram, and green gram respectively. Whereas, the negative RI of black gram (-0.677) and green gram (-0.125) of shoot length, rice (-0.080 and -0.016), and black gram (-0.817 and -0.384) of fresh weight and dr weight registered respectively. With regards to the highest RI of positive (+) values registered in the composted coir pith compared to the raw coir pit RI. (Table 3 and (Fi ure 2)

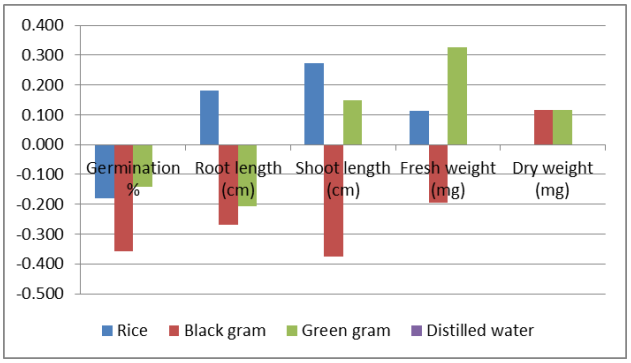

Figure 1: Response index values of composted coir pith on rice, black gram, and green

Table 3: Response index values for inhibition effect of rice, black gram, and green gram germination and seedling growth

Response Index of coir pith					
Coir pith RI	Germination %	Root length (cm)	Shoot length (cm)	Fresh weight (mg)	Dry weight (mg)
Rice	-0.226	-0.012	+0.077	-0.080	-0.016
Black gram	-0.425	-0.476	-0.677	-0.817	-0.384
Green gram	-0.271	-0.321	-0.125	+0.207	+0.203
Response Index of composted coir pith					
Rice	-0.179	+0.183	+0.273	+0.113	+0.000
Black gram	-0.357	-0.268	-0.376	-0.196	+0.117
Green gram	-0.143	-0.207	+0.150	+0.328	+0.116
Distilled water	0.00	0.00	0.00	0.00	0.00

The chemical class distributions of the coir pith extracts are summarized in Table 4 and the GCMS/MS Chromatogram in fig 3. The compounds were separated into eight classes: Acid, Alcohol, Alkane, Amide, Azo compound, Ester, Ketone, and Pyrimidine. Among the 29 chemical compounds, the alcohol class of Tocopherol showed severe seedling growth inhibition phenotype, suggesting that PC-8 functions as a lipid antioxidant in early plant development (Mène-Saffrané et al., 2010), and Fucoxanthin derived of strigolactone, has recently identified phytohormone involved in the inhibition of shoot branching of young plants, is also derived from carotenoids (Umehara et al., 2008; Gomez- Roldan et al., 2008; Seto et al., 2012). The alkane class of Tetramethyl Heptadecane and Dichloroacetamide inhibited leaf growth as induced by auxin was found to be independent of ethylene in common bean (Phaseolus vulgaris) plants (Keller, et al., 2004). The inhibition of ethylene by applying 1 mM ethylene synthesis inhibitor aminooxy acetic acid (AOA) with 1 mM IAA did not affect auxin-induced inhibition of leaf growth. The Azo compound of Tetrazole has been found useful as inhibitors of top growth for vegetables, fruit trees, cereals, and canes. Application of 5-amino tetrazole to the soil at planting time has caused temporary albinism in some plants and reduction of tetrazolium salts to red colored formmazans has been used to detect the activity of reducing enzymes in seeds. The Ester class of Hydroxyethyl palmitate is the derivation of N-Acylethanolamines (NAEs). The new phenoxyacylethanolamides may be able to enhance endogenous FAAH activity in wild-type seedlings, to confer some tolerance to the growth inhibition by NAE (Lionel Faure et al., 2014). The Ketone class of Neocurdione is a development of amine oxidase in the apical part was inhibited by administration of neocuproine, and this effect was markedly reversed by the addition of copper disodium ethylene diamine tetraacetate (EDTA-Na_2-Cu) (Yonezo Suzuki and Hiroshi Yanagisawa, 1976)

and the Pyrimidine class of Uridine is inhibition of potato tuber of de novo pyrimidine synthesis leads to a compensatory stimulation of the pyrimidine salvage pathway (Geigenberger *et al.*, 2005). The presence of the above bioactive compounds in the coir pith may act as an inhibitory agent for young plants like rice, black gram, and green gram.

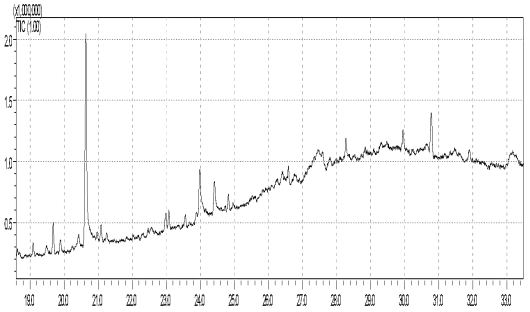

Figure 3: GCMS/MS Chromatogram of coir pith

Table 4: Chemical compounds in coir pith by GCMS/MS

S.No	Retention time	Area / Height (%)	Compound name	Compound class
1	20.643	3.82	n-Hexadecanoic acid	Acid
2	23.984	4.52	9-Octadecenoic acid, (E)-	Acid
3	24.419	5.45	Octadecanoic acid	Acid
4	27.935	4.51	Succinic acid, 1,1,1-trifluoropro	Acid
5	28.385	3.19	2-Bromopropionic acid, 6-ethyl	Acid
6	28.565	2.56	Doconexent, TMS derivative	Acid
7	29.586	5.27	.alpha.-Hydroxystearic acid	Acid
8	30.584	2.29	Fumaric acid, dodecyl 2-hexyl e	Acid
9	27.472	4.08	.alpha.-Tocopherol-.beta.-D-ma	Alcohol
10	27.655	2.49	Cholest-7-en-3-ol, 4,4-dimethyl	Alcohol
11	29.280	1.46	Fucoxanthin	Alcohol
12	29.759	2.62	Isofucosterol, O-TMS	Alcohol
13	22.992	3.88	Eicosane	Alkane
14	26.588	5.09	Octacosane, 1-iodo-	Alkane
15	27.591	7.42	4,8,12,16-Tetramethylheptadeca	Alkane
16	28.278	5.57	Eicosane	Alkane
17	29.952	6.30	Hexadecane, 2,6,10,14-tetramet	Alkane
18	27.804	4.06	Dichloroacetamide, N-nonyl-	Amide
19	28.620	2.85	Butyramide, 2-bromo-N-octyl-	Amide
20	27.780	2.28	Tetrazole, 5-[2-(1-perhydroazep	Azo compound
21	29.852	2.05	Methyl 2,3-dihydroxybenzoate,	Ester
22	30.046	4.01	Valtrate	Ester
23	26.864	2.87	2-Hydroxyethyl palmitate, TMS	Ester
24	26.029	4.00	Neocurdione	Ketone
25	27.185	1.77	Norbolethone	Ketone
26	29.255	2.22	2-Methyl-6-(5-methyl-2-thiazolidone	Ketone
27	29.479	2.06	Geldanamycin, 18,21-didehydro	Ketone
28	30.937	3.35	Dihydroartemisinin, 5-de hydro	Ketone

29	30.185	2.64	Uridine, 2',3'-O-(1-methylethyli	Pyrimidine

The chemical class distributions of the composted coir pith constituents extracts are summarized in Table 5 and the GCMS/MS Chromatogram of fig 4. The compounds were separated into seven classes: Acid, Alcohol, Aldehyde, Alkane, Amide, Ester, and Guanidine. Among the seven class compounds that mostly come under the characteristic feature of fatty acids is the carboxyl function. The composted coir pith while decomposition polyphenol content contains and phenolic compounds is less by degraded. The microorganisms can utilize and degrade polyphenols (Chan, 1986), and as many polyphenols are water-soluble nature coir pith. The composted coir pith has a low C: N ratio, which provides nutrients for crops (Bollen and Lu, 1957).

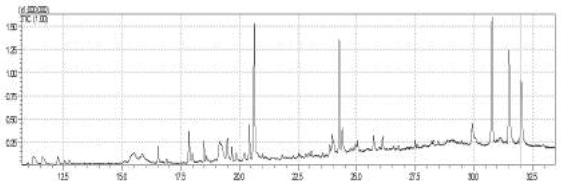

Figure 4: GCMS/MS Chromatogram of composted coir pith

Table 5: Chemical compounds in composted coir pith by GCMS/MS

S.No	Retention time	Area / Height (%)	Compound name	Compound class
1	12.256	4.13	Dodecanoic acid	Acid
2	16.532	3.06	Tetradecanoic acid	Acid
3	17.848	3.29	Pentadecanoic acid	Acid
4	18.494	2.74	1,2-Benzenedicarboxylic acid, b	Acid
5	20.211	3.25	Oleic Acid	Acid
6	20.630	3.56	n-Hexadecanoic acid	Acid
7	21.832	2.82	Eicosanoic acid	Acid
8	23.960	3.53	9-Octadecenoic acid (Z)-, 2,3-di	Acid
9	24.392	3.70	Octadecanoic acid	Acid
10	24.733	2.27	Acetic acid, chloro-, octadecyl e	Acid
11	27.900	3.45	Hydroxyvalerenic acid	Acid
12	30.615	6.04	Retinoyl-.beta.-glucuronide 6',3'	Acid
13	22.825	4.17	Behenic alcohol	Alcohol
14	22.966	3.13	7-Hexadecyn-1-ol	Alcohol
15	30.000	1.59	Perillaldehyde-O-methyloxime	Aldehyde
16	17.991	3.78	Docosanoic acid, 1,2,3-propane	Alkane
17	20.965	2.85	9-Hexacosene	Alkane
18	24.820	6.60	Decane, 5-ethyl-5-methyl-	Alkane
19	28.267	2.35	Hexacosane, 1-iodo-	Alkane
20	31.139	3.43	5-(7-Isopropyl-10-methyl-1-oxo	Alkane
21	24.030	4.01	Cyclohexanol, 1R-4cis-acetamid	Amide
22	29.946	3.90	Nonivamide	Amide
23	19.684	2.50	Hexadecanoic acid, methyl ester	Ester
24	20.425	2.93	Dibutyl phthalate	Ester
25	25.037	2.56	Eicosyl acetate	Ester
26	30.779	3.40	Bis(2-ethylhexyl) phthalate	Ester
27	26.790	3.06	n-Octyl guanidine	Guanidine

V. CONCLUSIONS

Despite numerous advantages and accessibility in huge amounts, coir substance is not completely used for gainful purposes due to the high C: N proportion (112: 1) and presence of the high amount of lignin. The use of raw coir pith with a wide C: N proportion can bring about immobilization of plant supplements. Also, polyphenols and phenolics acids can be phytotoxic and repress plant development, and hence it can be used for moisture conservation and other related works while composted coir pith can be used for various agricultural and horticultural works including nurseries. Besides, composted coir pith is also a good source of organic matter for agricultural use for soil health building.

ACKNOWLEDGMENTS

The authors wish to thank the Core Projects for research activities at College and Research stations of TNAU - Phase III (Post Doctoral Fellowships), funded by Agriculture Department, Govt. of Tamil Nadu, 2018 - 2021, Tamil Nadu Agricultural University, Coimbatore, India. Also, wish to thank the Department of Entomology, AC & RI, Madurai, TNAU for the laboratory facilities.

REFERENCES

1. Ayeni, A.O., D.T. Lordbanjou and B.A. Majek BA: Tithonia diversifolia (Mexican sunflower) in south-western Nigeria: occurrence and growth habit. Weed Research., 37, 443- 449 (1997).
2. Bhatt, B.P. and N.P. Todaria NP: Studies on the allelopathic effects of some agroforestry tree crops of Garhwal Himalaya. Agroforestry Systems., 12, 251-255 (1990).
3. Bollen, W.B. and K.C. Lu: Effect of Douglas-fir sawdust mulches and incorporations on soil microbial activities and plant growth. Soil Science Society of America Proceedings., 21(1), 35-41 (1957).
4. Bremmer, J.M. and C.S. Mulvaney: Nitrogen-total. In: Page, A.L., Miller, R.H., Keeney, D.R. (Eds.), Methods of Soil Analysis, Part 2. Chemical and Microbiological Properties, second ed., Agronomy series No. 9 ASA, SSSA, Madison (1982).
5. Chan, Y.K.:Utilization of simple phenolics for di nitrogen fixation by soil diazotmphlc bacteria. Plant Soil., 90, 141 -150 (1986).
6. Geigenberger, P., B. Regierer, A. Nunes-Nesi, A. Leisse, E. Urbanczyk-Wochniak, F. Springer, J.T. Van Dongen, J. Kossmann and A.R. Fernie: Inhibition of de novo pyrimidine synthesis in growing potato tubers leads to a compensatory stimulation of the pyrimidine salvage pathway and a subsequent increase in biosynthetic performance. Plant Cell., 17, 2077-2088(2005).
7. Gomez, K.A. and A.A. Gomez: Statistical procedures for agricultural research, 2nd Edn.; John Wiley Sons, New York (1984).
8. Gomez-Roldan, V., S. Fermas, P.B. Brewer, V. Puech-Pagès, E.A. Dun, J.P. Pillot, F. Letisse, R. Matusova, S. Danoun, J.C. Portais, H. Bouwmeester, G. Bécard, C.A. Beveridge, C.Rameau and S.F.Rochange SF: Strigolactone inhibition of shoot branching. Nature., 455, 189-194 (2008).
9. Gruda, N., B. Rau and R.D. Wright: Laboratory bioassay and greenhouse evaluation of a pine tree substrate used as a container substrate. Europ. Journal of Horticultural Science., 74(1), 73-78 (2009).
10. Keller, C.P., R. Stahlberg, L.S. Barkawi and J.D. Cohen JD: Long-term inhibition by auxin of leaf blade expansion in bean and Arabidopsis. Plant Physiology,. 134(3),1217-26 (2004).
11. Lemaire, F., A. Dartigues and L.M. Riviere: Physical and chemical characteristics of a lignocellulosic material. Acta Horticulturae., 238, 9-22 (1989).
12. Lionel Faure., Subbiah Nagarajan, Hyeondo Hwang, Christa L Montgomery, Bibi Rafeiza Khan, George John, Peter Koulen, Elison B Blancaflor and Kent D Chapman: Synthesis of Phenoxyacyl-Ethanolamides and Their Effects on Fatty Acid Amide Hydrolase Activity. Journal of Biological Chemistry., 289(13), 9340-9351 (2014).
13. Maher, M.J. and D. Thomson: Growth and Mn content of tomato (Lycopersicon esculentum) seedlings grown in Sitka spruce (Picea

sitchensis (Bong.) Carr.) bark substrate. Science of Horticulture., 48, 223-231 (1991).
14. Mène-Saffrané, L., A.D. Jones and D. Della Penna: Plastochromanol-8 and tocopherols are essential lipid-soluble antioxidants during seed desiccation and quiescence in Arabidopsis. Proc Natural Academic Science, USA 107: 17815-17820 (2010).
15. Morel, P. and G. Guillemain: Assessment of the possible phytotoxicity of a substrate using an easy and representative biotest. Acta Horticulturae., 64, 417-423 (2004).
16. Ortega, M.C., M.T. Moreno, J. Ordovas and M.T. Aguado: Behavior of different horticultural species in phytotoxicity bioassays of bark substrates. Science Horticultre., 66, 125-132 (1996).
17. Orwa, C., A.Mutua, R.Kindt, R. Jamnadass and S. Anthony: Agroforestree database: a tree reference and selection guide version 4.0. http://www.worldagroforestry.org (2009).
18. Penningsfeld, F.: Toresa a new substrate for soilless culture. Eighth Intl Congress on Soilless Culture. Hunter's Rest South Africa. ISOSC Proceedings p. 335-345 (1992).
19. Richardson, D.R and G.B. Williamson: Allopathic effects of shrubs of the sand pine scrub on pines and grasses of the sandhills. Forest Science., 34(3), 592- 605 (1988).
20. Seto,Y., H. Kameoka, S.Yamaguchi and J. Kyozuka: Recent advances in strigolactone research: chemical and biological aspectes. Plant and Cell Physiology., 53, 1843-1853 (2012).
21. Turk, M.A and A.M. Tawaha: Allelopathic effect of black mustard (Brassica nigra L.) on germination and growth of wild oat (Avena fatua L.). Crop Protection., 22, 667-673(2003).
22. Umehara, M., A. Hanada, S. Yoshida, K. Akiyama, T. Arite, N. Takeda-Kamiya, H. Magome, Y. Kamiya, K. Shirasu, K. Yoneyama and et al: Inhibition of shoot branching by new terpenoid plant hormones. Nature., 455, 195-200 (2008).
23. Williamson, G.B., D.R. Richardson and N.H. Fischer: Allelopathic mechanism in fire-prone communities," in Allelopathy. Chapman and Hall, London, UK pp. 59-75 (1992).
24. Yonezo Suzuki and Hiroshi Yanagisawa: Effect of neocuproine and cuprizone on the development of amine oxidase and growth in pea seedlings. Plant and Cell Physiology., 17 (6), 1359-1362 (1976).